



**UNIVERSITÀ DEGLI STUDI DI SALERNO**

**Dipartimento di Chimica e Biologia "A. Zambelli"**

**Dottorato di Ricerca  
in  
*Chimica*  
XXXIV Ciclo**

**Doctoral Thesis**

**Copolymerization of olefins with polar monomers by  
transition metal catalysts**

**Tutor and Ph.D. Coordinator**

Prof. Claudio Pellecchia

**Ph.D. student**

Zeinab Saki

## Table of Contents

Chapter 1 .....	7
<b>Introduction</b> .....	7
<b>1.1 Polyolefins</b> .....	7
<b>1.2 Copolymerization of ethylene</b> .....	9
<b>1.4 General Mechanism for polymer formation</b> .....	11
<b>1.3 Types of Catalyst</b> .....	12
Early transition metal catalyst.....	12
late transition metal catalyst .....	13
<b>Palladium and Nickel Metal Catalysts for Polymerization Studies</b> .....	14
<b>Ni-LTM catalysts based on bis imine ligands</b> .....	21
<b>Chapter 2</b> .....	25
<b>Results and discussion</b> .....	25
<b>2.1. Copolymerization of Ethylene and Methyl Acrylate by Pyridylimino Ni(II) Catalysts Affording Hyperbranched Poly(Ethylene-co-Methylacrylate)s with Tunable Structures of the Ester Groups</b> .....	25
<b>2.2. Copolymerization of Ethylene and Methyl Acrylate by Dibenzocycloheptyl-substituted Aryliminopyridyl Ni(II) catalysts</b> .....	50
<b>2.3. Iminopyridine Ni(II) catalysts affording either oily hyperbranched oligoethylenes or crystalline polyethylenes depending on the reaction conditions: possible role of in situ catalyst structure modifications</b> .....	67
<b>Chapter 3</b> .....	77
<b>EXPERIMENTAL PART</b> .....	77
<b>3.1 General Conditions</b> .....	77
<b>3.2 General procedure for ethylene homo- and copolymerizations at 6 atm</b> .....	78
<b>3.3 General procedure for ethylene-methyl acrylate copolymerization at higher pressures</b> .....	79

<b>3.4 Synthesis of ligands and complexes</b> .....	79
<b>CONCLUSION</b> .....	86

<b>Figure 1.</b> Global consumption of polyolefins comparison to other polymers [2017] ....	8
<b>Figure 2.</b> Different kinds of polyethylene .....	9
<b>Figure 3.</b> Obstacles for copolymerization of ethylene with vinyl polar monomer .....	11
<b>Figure 4.</b> General mechanism for polymer formation.....	11
<b>Figure 5.</b> Group 4 early transition metal catalyst.....	12
<b>Figure 6.</b> Activation of the early transition metal catalyst .....	13
<b>Figure 7.</b> General structures of Late Transition Metals .....	14
<b>Figure 8.</b> Cationic $\alpha$ -diimine catalyst.....	15
<b>Figure 9.</b> Copolymerization mechanism of methyl acrylate with Cationic $\alpha$ -diimine catalyst. ....	16
<b>Figure 10.</b> Examples of Pd-based precatalysts for the ethylene/polar vinyl monomer	17
<b>Figure 11.</b> Examples of Pd-based precatalysts for with different bulkiness. ....	18
<b>Figure 12.</b> Examples of Ni-based precatalysts for the ethylene/polar vinyl monomer copolymerization. ....	21
<b>Figure 13.</b> Mechanism of chain growth reactions of polyethylene by $\alpha$ -diimine catalysts.....	23
<b>Figure 14.</b> Synthesis of the Ni complexes <b>Ni1-Ni4</b> . ....	25
<b>Figure 15.</b> $^1\text{H}$ NMR spectra ( $\text{CDCl}_3$ , T = 298 K) of the copolymer sample of run 3...31	
<b>Figure 16.</b> Methoxy regions of the $^1\text{H}$ NMR spectra ( $\text{CDCl}_3$ , T = 298 K) of the copolymer samples of runs 2 (lower trace), 13 (middle trace) and 6 (upper trace). ....	32
<b>Figure 17.</b> Carbonyl, methoxy and C=O substituted methine regions of the $^{13}\text{C}$ NMR spectra ( $\text{CDCl}_3$ , T = 298 K) of copolymer samples of runs 3 (lower trace), 14 (middle trace) and 6 (upper trace). ....	33
<b>Figure 18.</b> $^{13}\text{C}$ -NMR spectrum ( $\text{CDCl}_3$ , T = 298 K) of copolymer sample 14 (Table 2) with enlargement of carbonyl region between 194-208 ppm. ....	34
<b>Figure 19.</b> $^1\text{H},^{13}\text{C}$ –HSQC spectrum ( $\text{CDCl}_3$ , T = 298 K) of sample 14 (Table 2). ....	35
<b>Figure 20.</b> Section of $^1\text{H},^{13}\text{C}$ –HMBC spectrum ( $\text{CDCl}_3$ , T = 298 K) of sample 14. $^1\text{H}$ scale: all the required signals; $^{13}\text{C}$ scale: carbonyl signals only, range 167 -178 ppm. ....	36
<b>Figure 21.</b> $^1\text{H},^{13}\text{C}$ –HSQC spectrum ( $\text{CDCl}_3$ , T = 298 K) of sample 16 (Table 2). ....	37
<b>Figure 22.</b> Section of $^1\text{H},^{13}\text{C}$ –HMBC spectrum ( $\text{CDCl}_3$ , T = 298 K) of sample 16. $^1\text{H}$ scale: signals at 12.42 and 12.24 ppm; $^{13}\text{C}$ scale: all the required signals. ....	38
<b>Figure 23.</b> Section of $^1\text{H},^{13}\text{C}$ HMBC spectrum ( $\text{CDCl}_3$ , T = 298 K) of sample 14. $^1\text{H}$ scale: all the required signals; $^{13}\text{C}$ scale: carbonyl signals only, range over 194 ppm. ....	39
<b>Figure 24.</b> Methoxy region of the $^1\text{H}$ NMR spectrum ( $\text{CDCl}_3$ , T = 298 K) of the copolymer sample 17 (Table 2). ....	43

<b>Figure 25.</b> Methoxy region of the $^1\text{H}$ NMR spectrum ( $\text{CDCl}_3$ , $T = 298\text{ K}$ ) of the copolymer sample 18 (Table 2). .....	44
<b>Figure 26.</b> $^{13}\text{C}$ NMR spectrum ( $\text{CDCl}_3$ , $T = 298\text{ K}$ ) of copolymer sample 18 (Table 2) with enlargement of carbonyl, methoxy and methine regions. ....	45
<b>Figure 27.</b> Dibenzocycloheptyl-substituted aryliminopyridyl Ni(II) complexes <b>5-9</b> ...	50
<b>Figure 28.</b> $^1\text{H}$ NMR spectra ( $\text{C}_6\text{D}_4\text{Cl}_2$ , $T = 298\text{ K}$ ) of the copolymer sample of entry 1. ....	52
<b>Figure 29.</b> $^1\text{H}$ NMR spectrum ( $\text{C}_6\text{D}_4\text{Cl}_2$ , $T = 353\text{ K}$ ) of the copolymer sample of entry 2. ....	53
<b>Figure 30.</b> $^{13}\text{C}$ NMR spectrum ( $\text{C}_6\text{D}_4\text{Cl}_2$ , $T = 353\text{ K}$ ) of the copolymer sample of entry 2. ....	54
<b>Figure 31.</b> DSC from the copolymer of entry 2 (Raw polymer). ....	55
<b>Figure 32.</b> $^1\text{H}$ NMR spectra ( $\text{C}_6\text{D}_4\text{Cl}_2$ , $T = 353\text{ K}$ ) of the pentane-insoluble fraction of the copolymer sample of entry 2. ....	56
<b>Figure 33.</b> $^1\text{H}$ NMR spectra ( $\text{CDCl}_3$ , $T = 298\text{ K}$ ) of the pentane-soluble fraction of the copolymer sample of entry 2. ....	56
<b>Figure 34.</b> $^1\text{H}$ NMR spectra ( $\text{C}_6\text{D}_4\text{Cl}_2$ , $T = 298\text{ K}$ ) of the copolymer sample of entry 3. ....	57
<b>Figure 35.</b> DSC from the copolymer of entry 3 (Raw polymer). ....	58
<b>Figure 36.</b> $^1\text{H}$ NMR spectrum ( $\text{CDCl}_3$ , $T = 298\text{ K}$ ) of the pentane-insoluble fraction of the copolymer sample of entry 3. ....	59
<b>Figure 37.</b> $^1\text{H}$ NMR spectra ( $\text{CDCl}_3$ , $T = 298\text{ K}$ ) of the pentane-soluble fraction of the copolymer sample of entry 3. ....	60
<b>Figure 38.</b> $^{13}\text{C}$ NMR spectrum ( $\text{CDCl}_3$ , $T = 353\text{ K}$ ) of the copolymer sample of entry 3. ....	61
<b>Figure 39.</b> $^1\text{H}$ NMR spectra ( $\text{CDCl}_3$ , $T = 298\text{ K}$ ) of the copolymer sample of entry 7. ....	62
<b>Figure 40.</b> $^1\text{H}$ NMR spectra ( $\text{CDCl}_3$ , $T = 298\text{ K}$ ) of the pentane-insoluble fraction of the copolymer sample of entry 7. ....	63
<b>Figure 41.</b> $^1\text{H}$ NMR spectra ( $\text{CDCl}_3$ , $T = 298\text{ K}$ ) of the pentane-soluble fraction of the copolymer sample of entry 7. ....	64
<b>Figure 42.</b> $^1\text{H}$ NMR spectra ( $\text{CDCl}_3$ , $T = 298\text{ K}$ ) of the copolymer sample of entry 8. ....	66
<b>Figure 43.</b> Iminopyridine Ni complexes <b>1-3,10</b> . ....	67
<b>Figure 44.</b> $^1\text{H}$ NMR ( $\text{CDCl}_3$ , $T = 298\text{ K}$ ) spectrum of oily fraction obtained in run 1, Table 6. ....	68

<b>Figure 45.</b> $^{13}\text{C}$ NMR ( $\text{CDCl}_3$ , $T = 298\text{ K}$ ) spectrum of oily fraction obtained in run 1, Table 6. ....	68
<b>Figure 46.</b> $^1\text{H}$ NMR ( $\text{CDCl}_3$ , $T = 293\text{ K}$ ) spectra of the products of reaction between complex 12 and $\text{AlEt}_2\text{Cl}$ under ethylene pressure. ....	71
<b>Figure 47.</b> $^1\text{H}$ NMR ( $\text{CDCl}_3$ , $T = 293\text{ K}$ ) spectra of the products of reaction between complex 1 and $\text{AlEt}_2\text{Cl}$ under ethylene pressure. ....	72
<b>Figure 48.</b> $^1\text{H}$ NMR ( $\text{CDCl}_3$ , $T = 293\text{ K}$ ) spectrum of the products of reaction between complex 1 and $\text{AlEt}_2\text{Cl}$ under nitrogen atmosphere, without ethylene. ....	73
<b>Figure 49.</b> Synthesis of the Ni-complexes Ni1-Ni4. ....	83
<b>Figure 50.</b> HR ESI Mass spectrum of complex <b>Ni1</b> ( $\text{L}^1\text{NiBr}_2$ ). ....	83
<b>Figure 51.</b> HR ESI Mass spectrum of complex <b>Ni2</b> ( $\text{L}^2\text{NiBr}_2$ ). ....	84
<b>Figure 52.</b> HR ESI Mass spectrum of complex <b>Ni3</b> ( $\text{L}_3\text{NiBr}_2$ ). ....	84

# Chapter 1

## Introduction

### 1.1 Polyolefins

Polyolefins are among the most widely used materials, with chemical and physical qualities such as stiffness, flexibility, and ductility, as well as a low cost of monomers, accounting for more than half of all thermoplastic polymers produced [1]. Crystalline plastics have specific melt temperatures ( $T_m$ ) or melting points. Amorphous plastics do not. They have softening ranges that are small in volume when solidification of the melt occurs or when the solid softens and becomes a fluid type melt. They start softening as soon as the heat cycle begins [2].

Among the various polyolefins, polyethylene (PE) has the biggest manufacturing volume, which began in the early 1930s with the production of low density polyethylene (LDPE) [1]. HDPE, LDPE, and LLDPE are the three basic kinds of polyethylene. HDPE is a low-branched polyethylene with a low flexibility ( $d=0.941 \text{ g/cm}^3$ ) produced by the Zeigler-Natta catalyst system. Although HDPE has a lower impact resistance than LDPE, it has a good resistance to chemical compounds, making it suitable for industrial applications such as fuel storage tanks, chairs, toys, and high-pressure water pipes. Another form of polyethylene known as UHMWPE is produced in smaller quantities than the others. The production of this type is more difficult than the others [2].

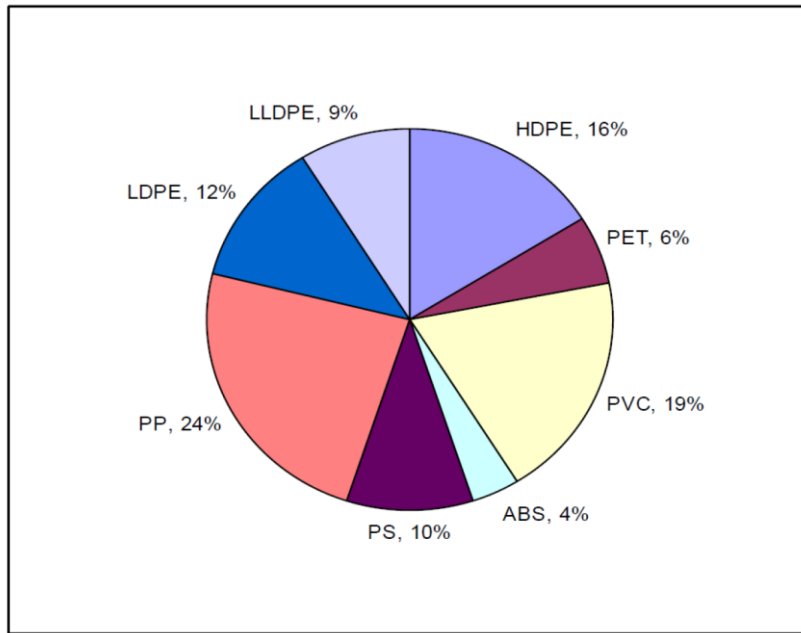


**Figure 1.** Global consumption of polyolefins comparison to other polymers [2017]

Low-density polyethylene (LDPE) is a branched polyethylene with a low crystallinity ( $d=0.910-940 \text{ g/cm}^3$ ) produced by free radical homopolymerization at high pressure and temperature. LLDPE stands for linear low-density polyethylene, which is made by copolymerizing ethylene with long-chain olefins using the Zeigler-Natta catalyst. These materials have a variety of features, including a low dielectric constant, good processability, and low cost [2].

Density, Melt Flow Index (MFI), and Molecular Weight Distribution are the most essential parameters of industrial polyethylene [2].



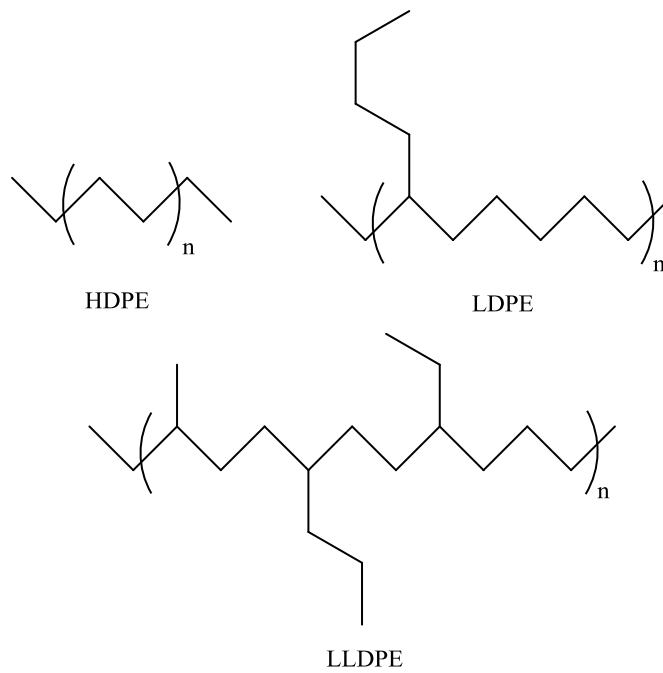


**Figure 2.** Different kinds of polyethylene

## 1.2 Copolymerization of ethylene

One of polyethylene's industrial constraints is the lack of polar groups in the structure, results in poor adhesion and anti-electricity properties, restricting the applications of these materials. Block copolymers and graft polyethylene can be used to mediate polyolefin interactions with other materials [18].

Modified polyolefins with good printability and adhesion qualities can be used in the film and printing industries [19].

Production of functionalized polyolefins by copolymerization or post-polymerization procedures is a challenging topic that is continuously being investigated [18].

Nevertheless, a sequence of reactions known as the "polar monomer problem" has prohibited the copolymerization of polar monomers is discussed in Figure 3. The first barrier is the deactivation of the metal center by strongly binding monomers, which might result in the production of metal-alkyl chelates, which are often ineffective catalysts. Another challenge is beta-x elimination, in which metal-x species (where x can be any heteroatom) are potential side products, leading deactivated catalytic species once again. The next issue is the misalignment of the monomer's energies with the border orbitals of catalyst [19].

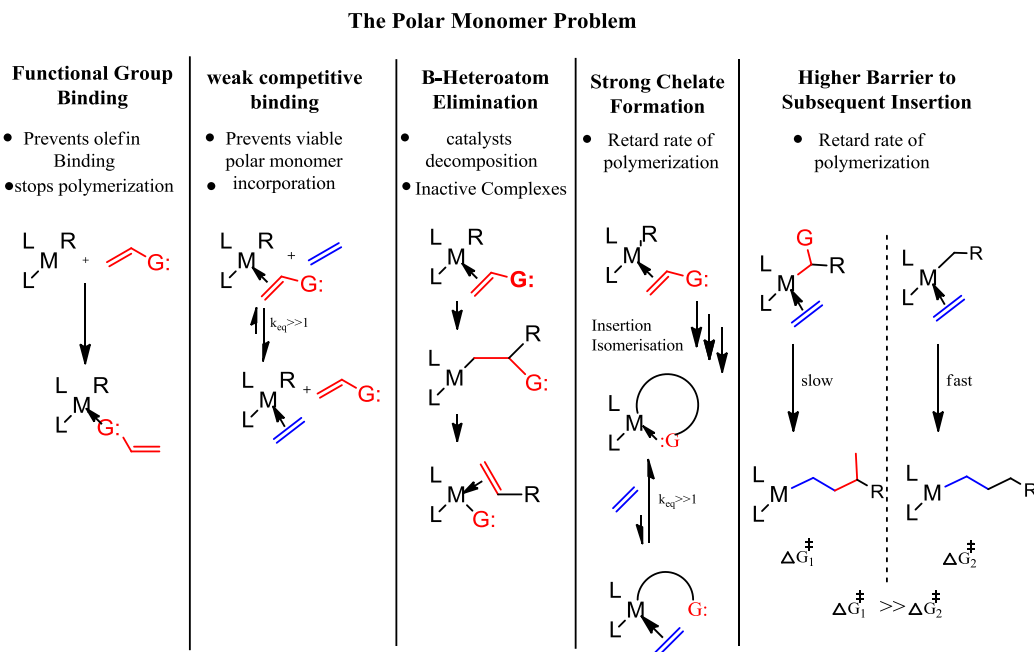


**Figure 3.** Obstacles for copolymerization of ethylene with vinyl polar monomer

### 1.4 General Mechanism for polymer formation

In general, polymerization has three steps: initiation, chain growth, and chain transfer, which begins with the insertion of ethylene into the transition metal active center. The activated monomer is then introduced into the transition metal-carbon bond to initiate chain growth. A chain transfer occurs at the conclusion, and a new chain begins [21] (Figure 4).

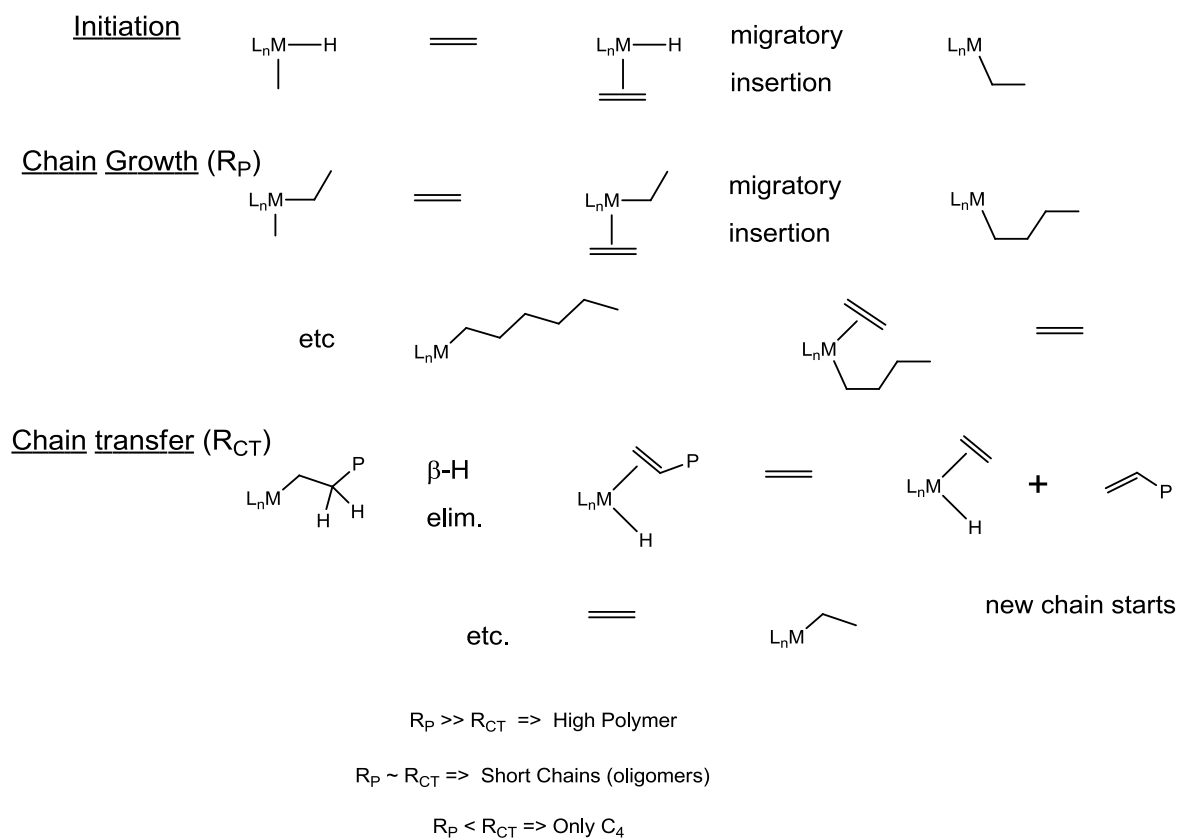


**Figure 4.** General mechanism for polymer formation.

### 1.3 Types of Catalyst

To polymerize olefins, transition metal catalysts are utilized. The two types of catalysts are late transition metals (LTM) and early transition metals (ETM) [18-20].

#### Early transition metal catalyst

The most practical catalysts for homopolymerization of ethylene are Ziegler catalysts. In the presence of polar monomers, these catalysts are ineffective. Because early transition metals are oxophilic, polar monomers deactivate the metal center and poison the catalyst, preventing it from being inserted [21]. The group 4 early transition metals of the form  $Cp'_2MR_2$  [21] is one of the most studied systems in coordination polymerization. Figure 5 shows this catalyst.

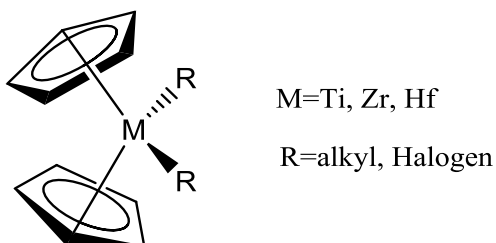


**Figure 5.** Group 4 early transition metal catalyst

These group 4 metal centers can be activated by alkylation of dihalide early transition metal catalysts with alkyl aluminum compounds (Figure 6a) [21].

An extracting factor for removing the alkyl from the metal can be used on the hand for activating the metal center of the dialkyl early transition metal catalyst (Figure 6b) [22].

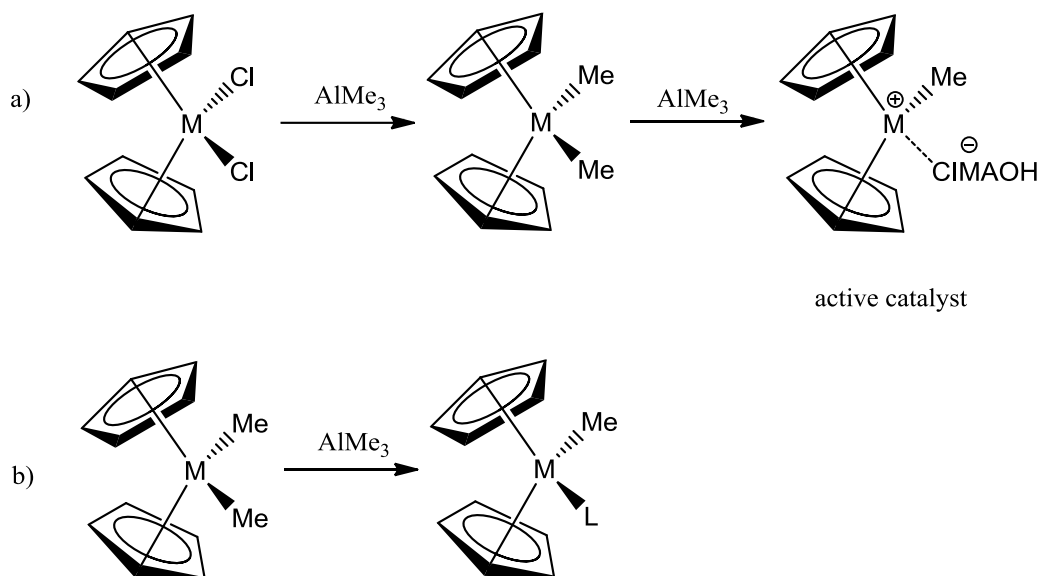


**Figure 6.** Activation of the early transition metal catalyst

### late transition metal catalyst

The first group of catalysts includes those consisting of iron, cobalt, nickel, platinum, palladium, and ruthenium. The alpha-diimine ligands of the first group of catalysts were developed by Brookhart. Highly branched polyethylene is produced by LTM catalysts [18-22].

At the same time as Brookhart, Gibson created the second breakthrough using late transition metal catalysts for ethylene polymerization, and it was related to ligands based on bis(imino)pyridyl. These catalysts produced high density linear low branching polyethylene based on the ligand. The presence of bulky ligands on iminoaryl rings has a significant impact on the molecular weight of the resultant polymers [18, 19].

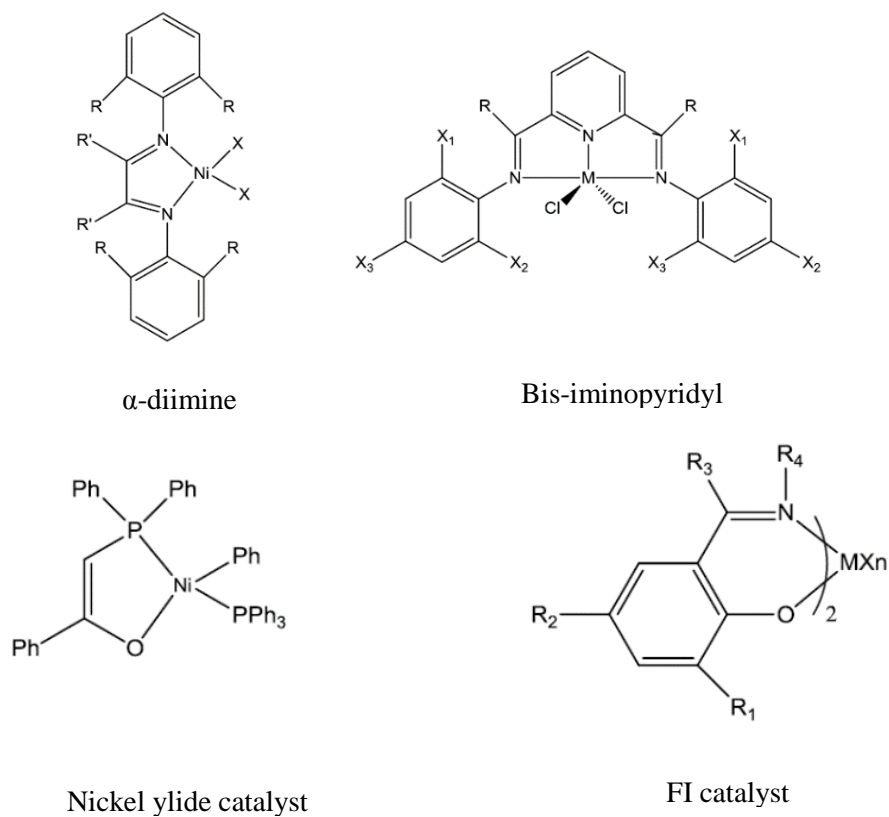


**Figure 7.** General structures of Late Transition Metals

In 1998, Fujita of Mitsui introduced a novel class of extremely active catalysts based on bulky phenoxy-imine and an early transition metal catalyst [18, 19]. These catalysts have unique structures and can create large amounts of polymers [20, 21].

### **Palladium and Nickel Metal Catalysts for Polymerization Studies**

Late metal catalysts are possible options for polar monomer insertion. The Brookhart and Gibson late metal catalysts, based on nickel and palladium, are

less electrophilic than their early metal counterparts and are able to tolerate polar monomers more effectively.

$[\text{PdMe}(\text{L})(\alpha\text{-diimine})]^+$  (1: L = solvent or neutral ligand, Figure 8) cationic  $\alpha$ -diimine complexes have been found to be effective catalysts for polymerization and copolymerization of ethylene with acrylates and methacrylates [1].

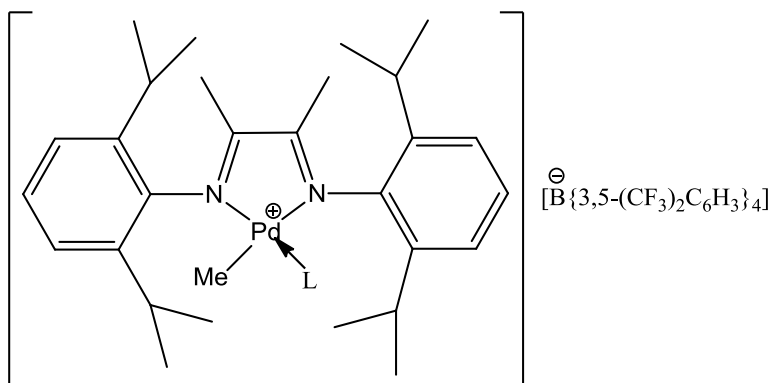


**Figure 8.** Cationic  $\alpha$ -diimine catalyst

Figure 9 shows the copolymerization mechanism for this system.

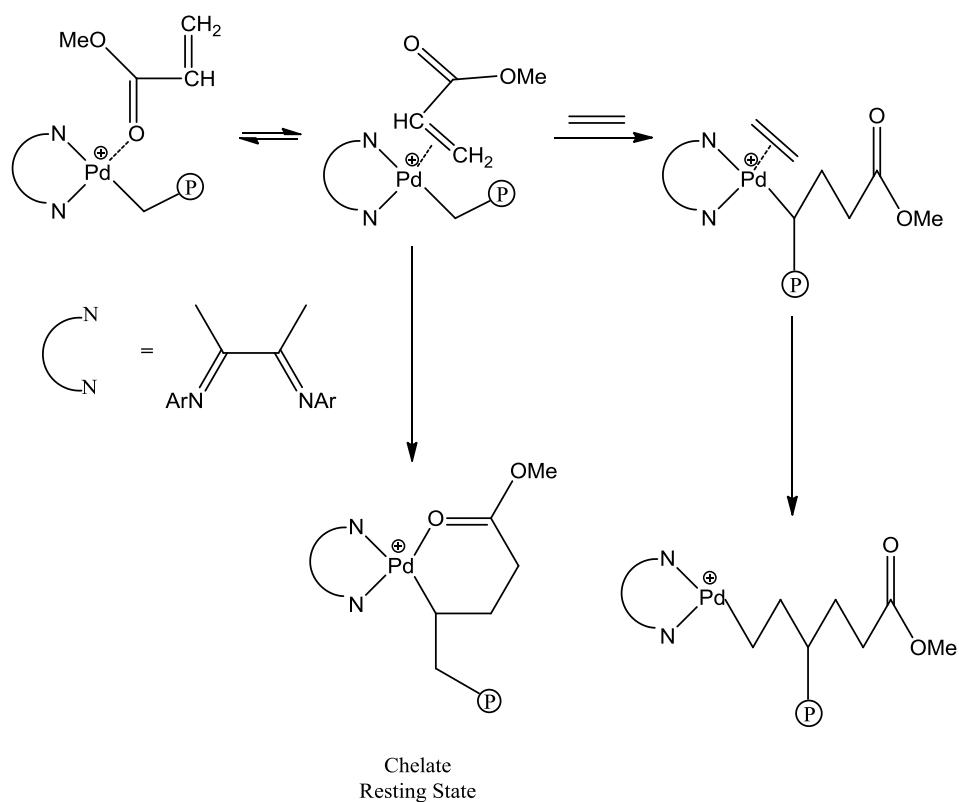


**Figure 9.** Copolymerization mechanism of methyl acrylate with Cationic  $\alpha$ -diimine catalyst.

Numerous Pd complexes belonging to the two classes have been produced and evaluated with a diversity of ligand variations. Varieties of the alpha-diimine family are relevant to the ligand skeleton, desymmetrization, and bulkiness of the ligand. For example compounds based on camphyl (Figure 10, A) [2] and dibenzobarrelene (Figure 10,B) [3] were used to produce thermally resistant catalysts for the live copolymerization of ethylene with MA, resulted in copolymers of various topologies relying on the ethylene pressure.



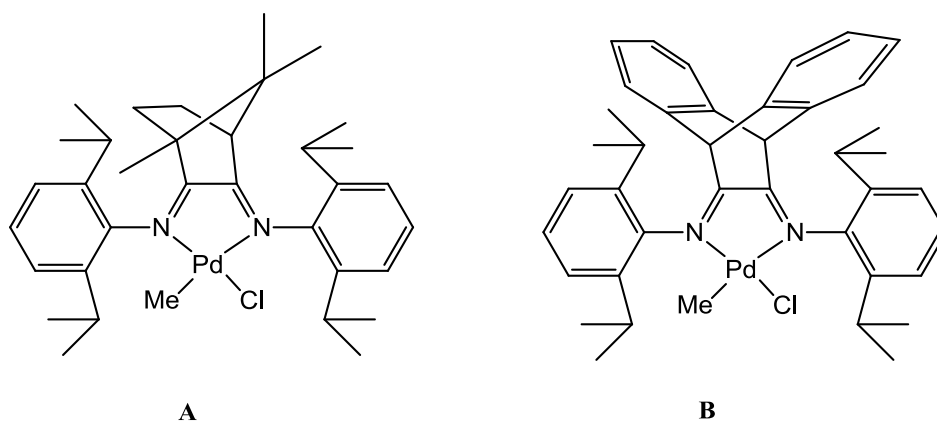


**Figure 10.** Examples of Pd-based precatalysts for the ethylene/polar vinyl monomer copolymerization.

Hyperbranched copolymers were indeed obtained at low pressure, whereas more linear macromolecules were produced at high pressure. Ligand desymmetrization consisted in differentiating the aryl rings on the two nitrogen atoms, mainly by the introduction of substituents of different steric hindrance [4, 5]. A few examples creating a subtle electronic and steric unbalance on the two nitrogen-donor atoms were reported resulting, in some cases, in better performing catalysts with respect to the corresponding symmetrical counterparts [6-8]. The importance of bulkiness around the catalytic center, pointed out by Brookhart since the first studies [9] was further exploited by using either “sandwich” palladium complexes (Figure 11, A) [10] or pentiptycenylium-substituted diimines (Figure 11, B) [11], or xanthene-bridged diimines (Figure 11, C) [12].

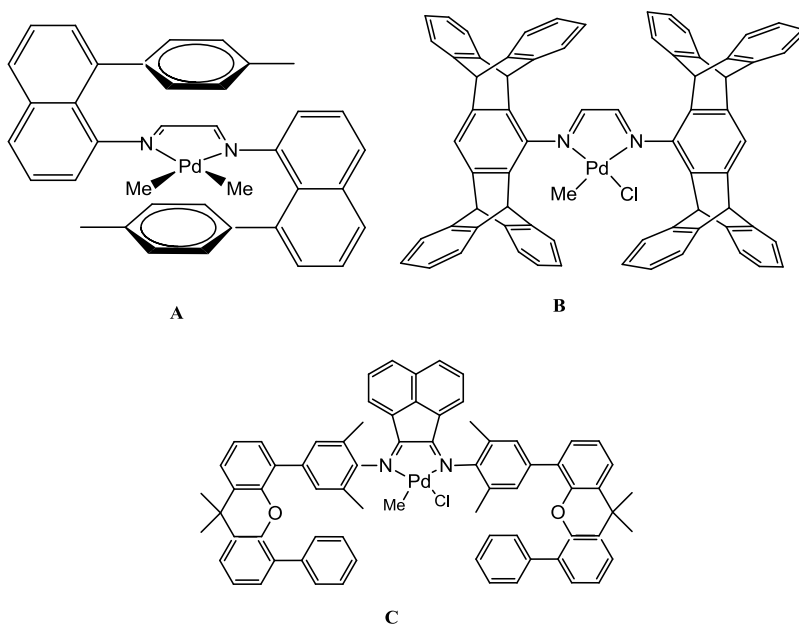


**Figure 11.** Examples of Pd-based precatalysts for with different bulkiness.

The first catalyzes the living copolymerization of ethylene with MA, whereas the second leads to E-MA copolymers of lower molecular weight and a higher content of inserted polar monomer with respect to the dibenzhydryl counterpart, indicating that the increased rigidity introduced in the ligand does not result to an increase in the steric hindrance on the axial positions of palladium. A first example of a dinuclear complex was based on a double decker diimine ligand in which the two bidentate compartments are connected by a xanthene fragment. Thanks to the peculiarity of this structure, E-MA copolymers having the polar monomer both in the main chain and at the end of the branches were obtained for the first time as the result of a cooperative effect between the two adjacent palladium centers [13].

The wide family of phosphine-sulfonate ligands mainly comprises molecules differing for the substituents on the non chelating P-aryl rings [14]. When these substituents are hydroxyl groups, it is possible to covalently bound the corresponding Pd-complex to carboxyl-functionalized polystyrene leading to the first E-MA copolymerization supported catalyst [14]. The obtained copolymers have a linear microstructure with a remarkably lower incorporation of the polar monomer with respect to the relevant molecular catalyst. Phosphine-sulphonate ligands with bulky alkyl groups on the phosphorus donor atom were also investigated and the corresponding Pd-catalyst led to E-polar vinyl monomer copolymers of high molecular weight, up to 177000 g/mol, that were not possible to obtain with the classical ligands of this class [15].

In comparison to the various literatures on Pd-based catalysts, examples of Ni peers are much harder to obtain and, in some cases, limited to the copolymerization of some specific polar monomers, as it is the type with the first salicylaldimine-nickel catalyst reported by Grubbs in 2000 that is capable of copolymerizing ethylene with inserted norbornenes (Figure 7, complex A) [16].

Brookhart and Daugulis recently reported that well-defined cationic [ $\alpha$ -diimine-NiMe(L)]<sup>+</sup> catalysts (perhaps synthesized in situ by activating [ $\alpha$ -diimine-NiBr<sub>2</sub>]) copolymerize with combinations of AlMe<sub>3</sub> and B-based ionizing factor including as B(C<sub>6</sub>F<sub>5</sub>)<sub>3</sub> and [Ph<sub>3</sub>C][B(C<sub>6</sub>F<sub>5</sub>)<sub>4</sub>] (Figure 7, complex B) [17]. Chen observed similar activity using sterically encumbered Drent-type phosphine-sulfonate or phosphine phosphonic amide Ni catalysts, whereas Nozaki observed similar behavior using N-heterocyclic carbene-quinolinolate Ni catalysts (Figure 12, complexes C-E) [18]. Shimizu et al. accomplished effective

copolymerization of ethylene with a variety of vinyl polar monomers, such as methyl acrylate catalyzed by bis(aryl)phosphinophenolate Ni(II). Notably are Chen's diphosphazane monoxide ligands, which provide either Pd or Ni catalysts for ethylene-acrylates copolymerization (Figure 12, complex G) [19].

Recently Pellecchia et al [20] discovered that activating the pyridylimino complex H (Figure 12) with  $\text{AlEt}_2\text{Cl}$  results in hyperbranched low molecular weight polyethylene. Steric bulkiness at the ortho position of the pyridine molecule drastically alters ethylene coordination, preferring chain transfer and chain walking over propagation.

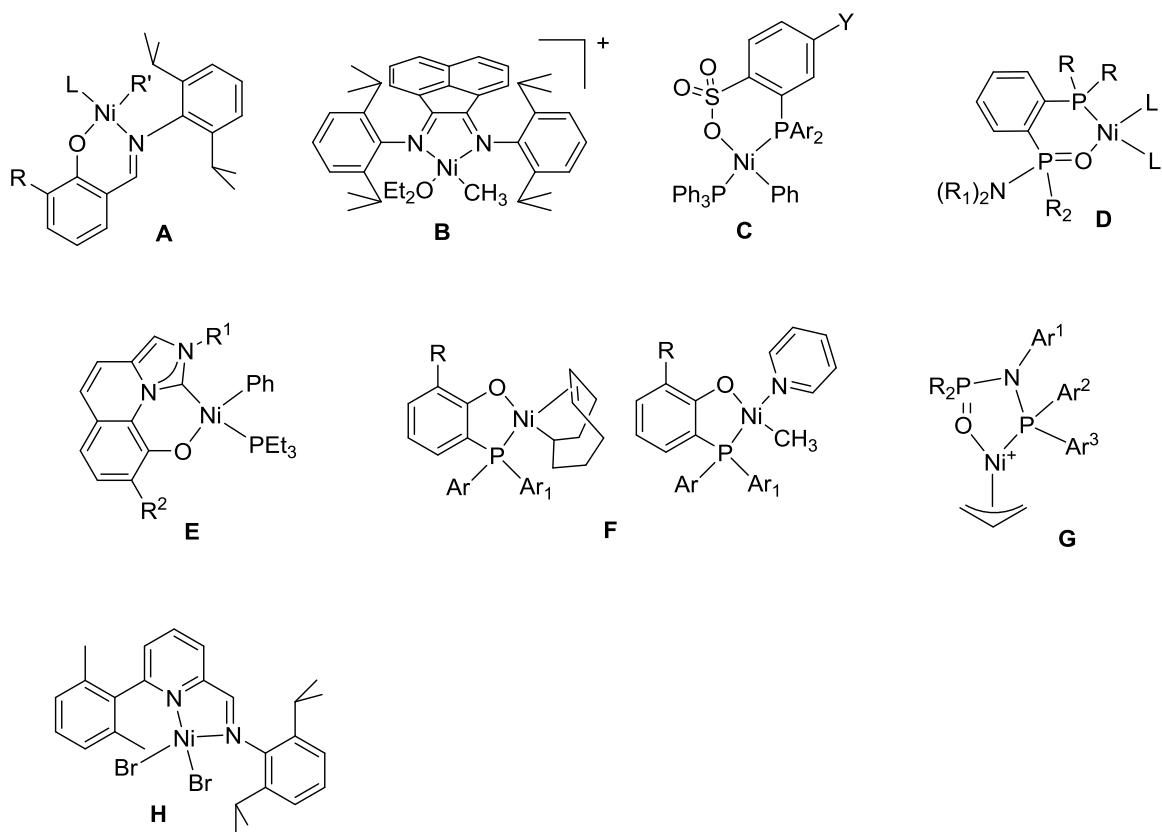


**Figure 12.** Examples of Ni-based precatalysts for the ethylene/polar vinyl monomer copolymerization.

### Ni-LTM catalysts based on bis imine ligands

Bulky ligands, particularly diimine, are found in the structures of LTM catalysts. Nickel, palladium, and platinum are commonly used to make these catalysts. The substituent R plays an essential role in the polymerization reaction, as it contributes to the formation of oligomers when groups with low impediment, such as hydrogen, methyl, and ethyl, are placed in the R position. By substituting

R for bulky substituents as isopropyl, tert-butyl and aryl, large molecular weight polymers can be obtained [18-21].

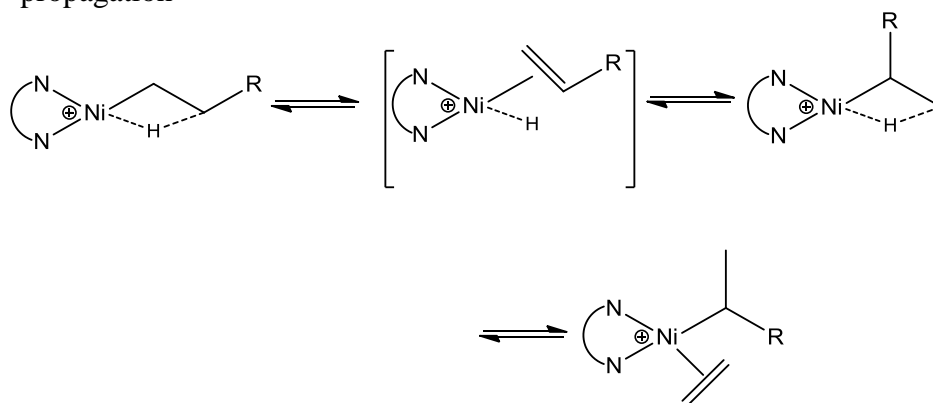
LTM catalysts have less electrophilicity than Ziegler-Natta and metallocene, allowing them to react with molecules containing free electron pairs. Compounds having a free electron pair, on the other hand, deactivate both catalysts. As a result, in the presence of LTM catalysts, copolymerization of ethylene with polar monomers such as methyl acrylate, vinyl acetate, and carbon monoxide is possible [15, 22, 23]. These catalysts are stable in the presence of polar monomers [24, 25]. The characteristics of plastic polyolefins alter dramatically when olefins containing polar monomers are added. Incorporating 5-20% polar monomers such as methyl acrylate, acrylic acid, and acrylonitrile into the polymer chain restores characteristics such as wettability, printability, and hardness [15] [22] and [26].

It's worth noting that chain isomerization can occur during the polymerization process. Depending on the reaction conditions and the type of catalyst, LTM catalysts can create branched polyethylene during chain walking polymerization. The first stage in this process is to eliminate the  $\beta$ -hydride, after that a polymer chain from the metal center develops by ethylene. After that, migratory insertion takes place, and a branch forms on the chain as it grows. Following that, propagation continues, resulting in a longer chain. The existence of branches from methyl to hexyl (Figure 13) is defined by the number of isomerization that occurs one after the other (Figure 13) [18, 19].

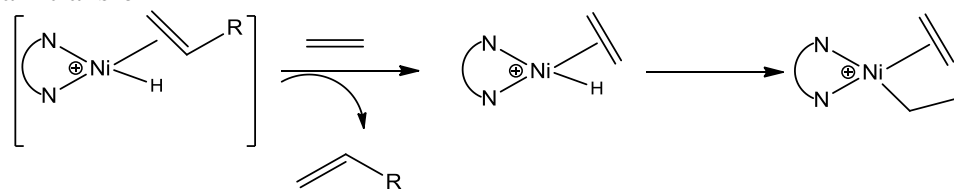
Polyethylene generated by LTM catalysts have a wide range of properties, from branching amorph to linear crystalline polymers. The structure of the catalyst (metal and kind of diimine ligand) as well as the polymerization conditions

(temperature and pressure) influence these qualities. For example, increasing the ethylene pressure reduces the number of branches in a specific catalyst structure.

a) propagation



b) chain transfer



C) Coordinated  $\beta$ -Hydrogen transfer for binding to the monomer

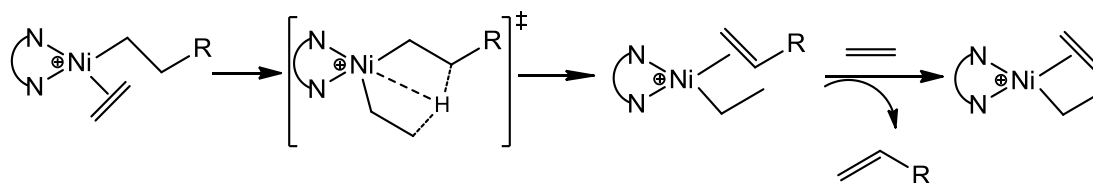


**Figure 13.** Mechanism of chain growth reactions of polyethylene by  $\alpha$ -diimine catalysts

The quantity of branching increases as the temperature rises. The competition between chain transfer and chain walking causes these effects. Branched polyethylene is used in the production of plastic materials, and it has recently received a lot of attention. Since tensile strength, impact strength, and flexibility of highly branched or linear polyethylene changes, they offer some advantages over high-density polyethylene [20-23].

The most significant distinction between palladium and nickel catalysts, including alpha-diimine ligands with Ziegler-Natta and metallocene catalysts, is the formation of branching microstructures from polar monomers.

Metal and ligand in LTM catalysts are capable of chain walking reactions. In comparison to Pd-based catalysts, the chain walking reaction is less effective in Ni-based catalysts. As a result, these catalysts form polymers with side chains, particularly methyl groups, ranging from low density to high density polymers [15, 18-20].



## Chapter 2

### Results and discussion

#### 2.1. Copolymerization of Ethylene and Methyl Acrylate by Pyridylimino Ni(II) Catalysts Affording Hyperbranched Poly(Ethylene-co-Methylacrylate)s with Tunable Structures of the Ester Groups

The pyridylimino proligands were synthesized following previously reported procedures [28]. The nickel complexes **Ni1-Ni4** were obtained, in about 90% yields, by allowing to react (dimethoxyethane)nickel dibromide and a slight excess of the proper ligand in methylene chloride, at 25 °C for 24 hours (Figure 14).

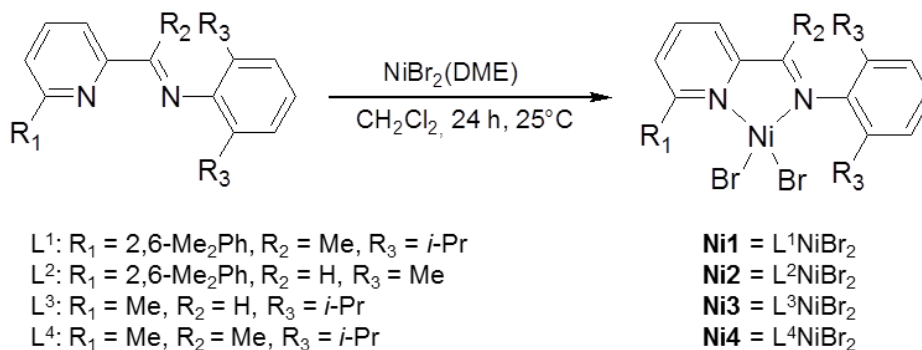


**Figure 14.** Synthesis of the Ni complexes **Ni1-Ni4**.

The **Ni1-Ni4** complexes were tested firstly in the homopolymerization of ethylene after activation with AlEt<sub>2</sub>Cl (200 equiv) under 6 atm monomer pressure

at 40 °C obtaining hyperbranched low molecular weight polyethylene oils. Afterwards all complexes were tested in the copolymerization of ethylene and methyl acrylate, after activation with 200 equiv of AlEt<sub>2</sub>Cl, at 40 °C, under different conditions of ethylene pressure and methyl acrylate concentrations. The complexes preliminary were checked under 6 atm of ethylene and different amounts of MA (Table 1). The complexes were characterized by <sup>13</sup>C and <sup>1</sup>H NMR and GPC analysis. In all cases they acquired oily products after pouring into the acidified methanol and then recovered with hexane/water.

The catalyst activities depend on steric bulkiness of the ligands. The highest activity observed for the complex **Ni1** with more hindrance as compared to other complexes. Subsequently the complex **Ni3** and **Ni4** have the lowest activity. Therefore, activities of the catalysts decrease in the order **Ni1** > **Ni2** > **Ni3** ~ **Ni4**. Consequently for the same amount of MA, [0.1] M, incorporation of Ni complexes is following the opposite trend as compared to the activity, 0.5 % for Ni1 to 1.5 % for Ni2 to 2.8 % for **Ni4** to 7.5 % for **Ni3** (Table 1, run 1-4), attributed to this fact that insertion and coordination of MA declines the polymerization reaction. On the other hand, increasing the amount of MA concentration in the reaction result in an increase of incorporation of MA but decrease of productivity (Table 1, runs 1 and 5). In run 5, double amount of MA, as compared to run 1, was used. As a result the amount of the obtained copolymer and activity reduced.

**Table 1.** Ethylene-methyl acrylate copolymerization by complexes **Ni1-Ni4** under 6 atm of ethylene<sup>a</sup>

Run (sample)	Ni catalyst	MA (mmol)	Yield (g)	Activity <sup>b</sup>	X <sub>MA</sub> <sup>c</sup> (mol%)	M <sub>n</sub> <sup>d</sup> (kDa)	PDI <sup>d</sup>	N <sub>br/1000</sub> <sup>e</sup>
1	<b>Ni1</b>	5	0.60	15	0.5	4.5	1.6	73
2	<b>Ni2</b>	5	0.16	4	1.5	0.7	2.3	98
3	<b>Ni3</b>	5	0.10	2.5	7.5	0.7	1.9	128
4	<b>Ni4</b>	5	0.10	2.5	2.8	1.0	1.2	77
5	<b>Ni1</b>	10	0.10	2.5	1.9	4.2	1.8	66
6 <sup>f</sup>	<b>Ni2</b>	5	0.30	7.5	6.1	0.8	1.6	125

<sup>a</sup>Polymerization conditions: Ni catalyst = 10 μmol dissolved in 2 ml of *o*-dichlorobenzene; cocatalyst = AlEt<sub>2</sub>Cl (2 mmol); solvent = 50 mL of toluene; T = 40 °C, P<sub>E</sub> = 6 atm, time 4 h.

<sup>b</sup>Activity in kg of copolymer/mol<sub>(Ni)</sub> h. <sup>c</sup>Incorporation of MA in the copolymer determined by <sup>1</sup>H NMR. <sup>d</sup>Determined by SEC vs polystyrene standards. <sup>e</sup>Determined by <sup>1</sup>H NMR. <sup>f</sup>Instead of AlEt<sub>2</sub>Cl, the cocatalyst was a mixture of AlMe<sub>3</sub> (1 mmol), B(C<sub>6</sub>F<sub>5</sub>)<sub>3</sub> (15 μmol)

Activation of catalysts with a combination of AlMe<sub>3</sub>/B(C<sub>6</sub>F<sub>5</sub>)<sub>3</sub>/[Ph<sub>3</sub>C][B(C<sub>6</sub>F<sub>5</sub>)<sub>4</sub>] as compared to the AlEt<sub>2</sub>Cl, transfers the catalyst to a highly active system for obtaining the copolymers [17, 18]. For this purpose, we performed a copolymerization reaction with AlMe<sub>3</sub> (1 mmol), B(C<sub>6</sub>F<sub>5</sub>)<sub>3</sub> (15 μmol) obtaining more incorporation of MA (run 6). The <sup>1</sup>H NMR spectra show that

copolymerization with  $\text{AlEt}_2\text{Cl}$  result in several peaks in the methoxy region while using the latter condition decreases selectivity in the mode of MA insertion.

Compared to samples produced by catalysts Ni1 with significant high molecular weight ( $M_n = 4.5$  kDa), molecular weights for samples produced by catalysts **Ni2** - **Ni4** are very low ( $M_n \leq 1$  kDa).

Additional runs at higher pressures and for a longer period of time were carried out in a stainless-steel autoclave, resulting in a variety of copolymers with varying properties (Table 2).

Subsequently, the catalysts were tested under the new condition. Under high pressure and using [0.25 M] of methyl acrylate, 10 and 30 atm of ethylene, complex **Ni1** produced a high amount of waxy copolymer which precipitated in acidified methanol (runs 7 and 8, Table 2). The obtained copolymers were branched polyethylene with low amount of methyl acrylate incorporation (0.2 % for sample 7 and 0.3% for sample 8). In the same condition of run 7, another run has been done without methyl acrylate resulting in 11g of oily polymer which was not precipitated in acidified methanol. Compared to the homopolymer, the copolymer had a higher molecular weight but lower branching. A possible explanation of these unexpected results is that, under these conditions,  $\kappa$ -O coordination of MA to the Ni catalyst site preferentially occurs vs  $\pi$ -coordination, disfavoring the  $\beta$ -agostic alkyl Ni intermediates which are precursors of both chain termination and chain running, thus resulting in polymers with less branching, higher molecular weight, and lower MA incorporation.

For catalyst **Ni2** under 30 atm of ethylene and [MA] = 0.25 M , 6.45 g of oily polymer was obtained with 0.3% of methyl acrylate incorporation (run 10, Table 2). With increasing methyl acrylate two times under the same pressure, the amount of methyl acrylate incorporation increased two times, but the yield decreased drastically (run 11, Table 2). In 10 atm of ethylene and 0.25 M of methyl acrylate a balance between the productivity and the incorporation of methyl acrylate was achieved (run 11, Table 2). In the same condition, with increasing the amount of methyl acrylate two times, a good incorporation of methyl acrylate was affordable but with decreasing of the productivity (run 13, Table 2).

The complex **Ni3** showed more tendency to methyl acrylate incorporation. The amount of incorporation of methyl acrylate reaching from 2.4% MA by applying MA = 0.125 M and 50 atm of ethylene to 17.7% MA by using 0.5M of methyl acrylate and 10 atm of ethylene but with low productivity (runs 14, 15, 16, Table 2).

**Table 2.** Ethylene-methyl acrylate copolymerizations by complexes **Ni1-Ni4** under higher ethylene pressure<sup>a</sup>

Run (sample)	Ni catalyst	MA (mmol)	P <sub>E</sub> (atm)	Yield (g)	X <sub>MA</sub> <sup>b</sup> (mol%)	M <sub>n</sub> <sup>c</sup> (kDa)	PDI <sup>c</sup>
7	<b>Ni1</b>	5	30	8.94 <sup>d</sup>	0.2	11.7	1.3
8	<b>Ni1</b>	5	10	5.32 <sup>d</sup>	0.3	9.3	1.4
9	<b>Ni1</b>	-	30	11.0	-	3.1	1.4
10	<b>Ni2</b>	5	30	6.45	0.3	1.2	1.7

11	<b>Ni2</b>	10	30	0.17	0.6	0.9	1.7
12	<b>Ni2</b>	5	10	1.04	1.2	1.1	1.5
13	<b>Ni2</b>	10	10	0.15	2.6	1.9	1.2
14	<b>Ni3</b>	5	30	0.14	7.8	0.3	1.1
15	<b>Ni3</b>	2.5	50	0.12	2.4	4.8	1.4
16	<b>Ni3</b>	5	10	0.10	17.7	0.3	1.0
17	<b>Ni3<sup>e</sup></b>	5	10	0.10	35.0	0.3	1.2
18	<b>Ni3<sup>f</sup></b>	5	30	0.17	11.0	0.3	1.1
19	<b>Ni4</b>	5	30	0.36	1.0	0.9	1.2

<sup>a</sup>Polymerization conditions: Ni catalyst = 10  $\mu$ mol dissolved in 2 mL of dichloromethane; cocatalyst = AlEt<sub>2</sub>Cl (2 mmol); solvent = 20 mL toluene; T = 40 °C, time 20 h. <sup>b</sup>Incorporation of MA in the copolymer determined by <sup>1</sup>H NMR. <sup>c</sup>Determined by GPC vs polystyrene standards. <sup>d</sup>A waxy polymer precipitated when the reaction mixture was poured into methanol; only traces of the oily fraction was recovered from the methanol solution. <sup>e</sup>Instead of AlEt<sub>2</sub>Cl, the cocatalyst was a mixture of AlMe<sub>3</sub> (1 mmol), B(C<sub>6</sub>F<sub>5</sub>)<sub>3</sub> (15 $\mu$ mol) and [Ph<sub>3</sub>C][B((C<sub>6</sub>F<sub>5</sub>)<sub>4</sub>)] (15 $\mu$ mol). <sup>f</sup>The Ni catalyst was dissolved in 2 mL of o-dichlorobenzene instead of dichloromethane.

Some runs were performed by activation with AlMe<sub>3</sub>/ B(C<sub>6</sub>F<sub>5</sub>)<sub>3</sub>/ [Ph<sub>3</sub>C][B(C<sub>6</sub>F<sub>5</sub>)<sub>4</sub>] instead of AlEt<sub>2</sub>Cl, obtaining copolymers with higher amount of methyl acrylate. For catalyst **Ni3** and **Ni2** in this condition as compared to the previous type of activation, incorporation reached to the 35% (run 17, Table 2) and 1.5 , 6% respectively (runs 2 and 6, Table 1). Catalyst **Ni4** did not show too much tendency to methyl acrylate but resulting in a higher yield (runs 14 and 19, Table 2).

Obtained products were analyzed by <sup>1</sup>H and <sup>13</sup>C NMR spectroscopy. The <sup>1</sup>H NMR spectrum of run 3 is showed in Figure 15. The spectrum is including

unsaturated vinylic, allyl and vinylidene protons and resonances of hyperbranched homo-PE as well [21]. A main broad peak is located at  $\delta$  3.67 which is related to the methoxy protons. By analyzing of this sample with  $^{13}\text{C}$  NMR, this peak is observed to be for in-chain inserted methoxy protons of MA (Figure 15)

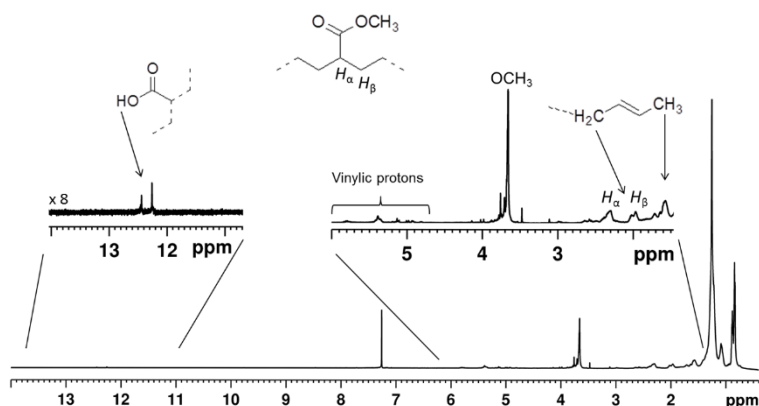


**Figure 15.**  $^1\text{H}$  NMR spectra ( $\text{CDCl}_3$ ,  $T = 298\text{ K}$ ) of the copolymer sample of run 3.

Two other resonances attributed to the methoxy regions were observed at  $\delta$  3.70 and 3.77 ppm. At the range of  $\delta$  2.20-2.66 and at 1.60 ppm, allylic protons and methylenic groups closer to the ester functionality are discovered. Minor low-field resonances are also detected between  $\delta$  12.24 and 12.42 ppm.

The  $^1\text{H}$  NMR spectra of runs 1-5 showed almost the same pattern, with main in-chain peak and two minor peaks in the methoxy region but only with different amounts of methyl acrylate incorporation, showing that the type of incorporation of methyl acrylate is independent from the kind of substituents located on pyridylimino ligand.

$^1\text{H}$  NMR analysis for other samples shows different result. The intensities of the three main peaks for methoxy groups differ remarkably (Figure 16). In Figure 16,  $^1\text{H}$  NMR spectra of methoxy regions of three runs with complex **Ni2**, run 2 (Table 1), run 13 (Table 2), and run 6 (Table 1), are showed and compared. For run 2, the main peak appears at  $\delta$  3.67 which is related to the methoxy group inserted in-chain in polymer, whereas for sample 13 there are three peaks. For sample 6 the major peak is at  $\delta$  3.77 is attributed to the end-chain methoxy groups (Figure 16).

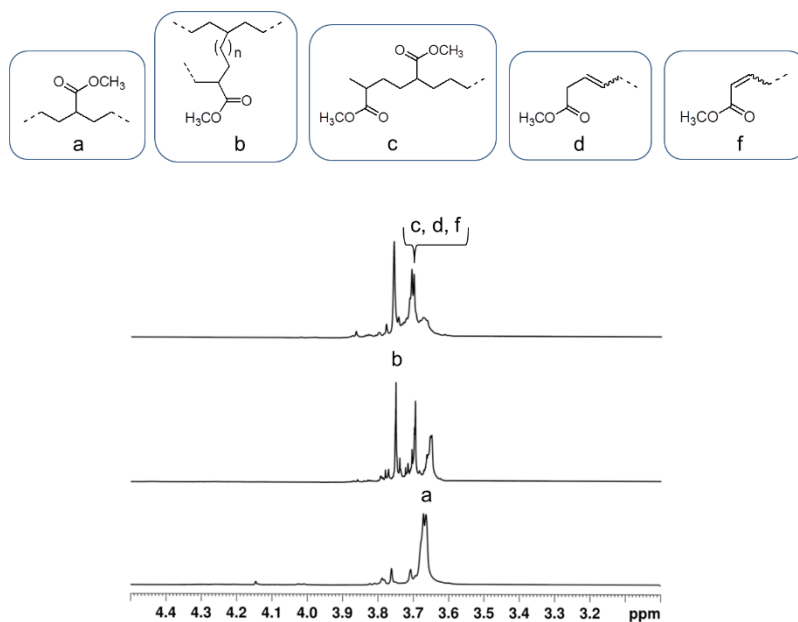


**Figure 16.** Methoxy regions of the  $^1\text{H}$  NMR spectra ( $\text{CDCl}_3$ ,  $T = 298\text{ K}$ ) of the copolymer samples of runs 2 (lower trace), 13 (middle trace) and 6 (upper trace).



As a result, the  $^{13}\text{C}$  NMR spectra for the various samples exhibit varied patterns of resonances. Figure 17 shows the carbonyl areas of three typical  $^{13}\text{C}$  NMR spectra, which are labeled according to the schemes.

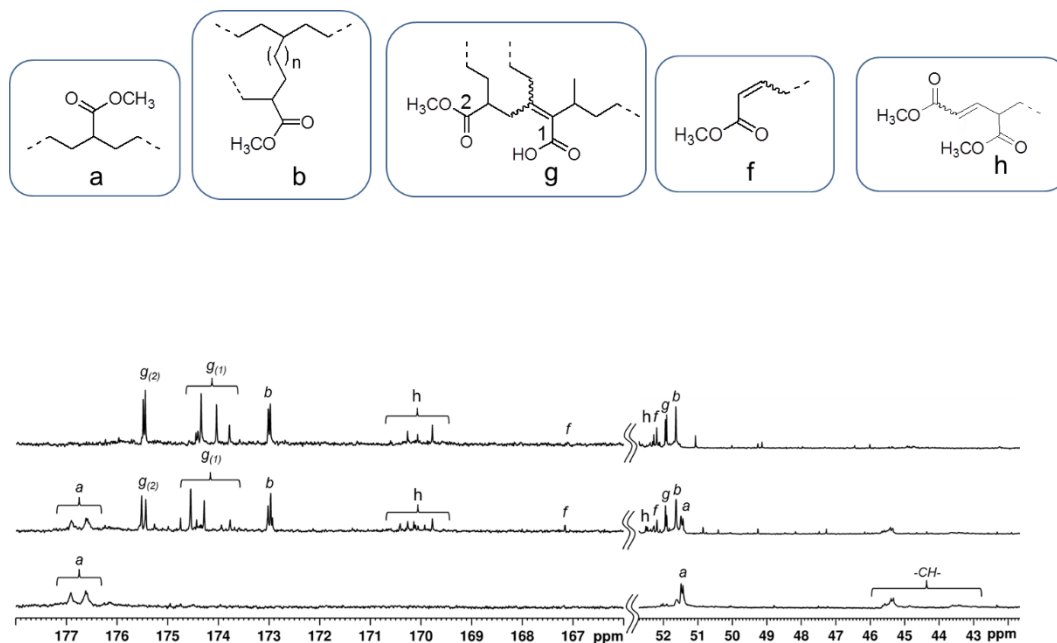


**Figure 17.** Carbonyl, methoxy and C=O substituted methine regions of the  $^{13}\text{C}$  NMR spectra ( $\text{CDCl}_3$ ,  $T = 298\text{ K}$ ) of copolymer samples of runs 3 (lower trace), 14 (middle trace) and 6 (upper trace).

Two large broad resonances are seen in the carbonyl area of the spectrum of sample 3 (Figure 17, lower trace) at 176.7 and 176.4 ppm; resonances at 51.5 ppm are assigned for the methoxy group, and at 45.4 and 43.6 ppm for the methine carbons of the MA units. These resonances are allocated to MA units inserted in-chain (fragment a) based on literature data and multidimensional

NMR tests: the existence of two broad resonances is likely owing to the macromolecules' hyperbranched structure and low  $M_w$ .

In addition to the peaks attributable to the MA units inserted in-chain stated above, more complex spectrum of the  $^{13}\text{C}$ -NMR of run14 (Figure 17, middle trace) are observed. Other four sharp resonances of corresponding intensities are observed at 175.5 (divided), 174.5, 174.3, and 173.0. (split). Between 170.4 and 169.8 ppm, as well as at 167.2 ppm, there are other less major peaks. There are partial peaks at 206.8, 205.7, and 194.9 (Figure 18).

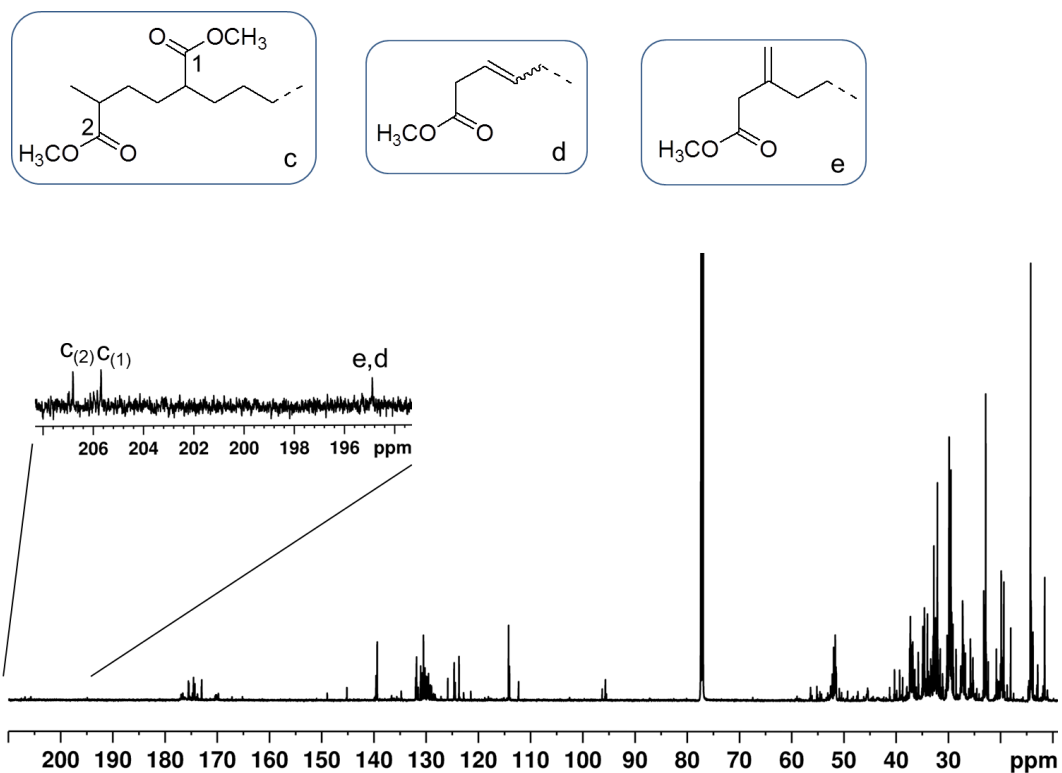


**Figure 18.**  $^{13}\text{C}$ -NMR spectrum ( $\text{CDCl}_3$ ,  $T = 298\text{ K}$ ) of copolymer sample 14 (Table 2) with enlargement of carbonyl region between 194-208 ppm.

It was feasible to identify the various segments containing the polar monomer on count of a detailed NMR investigation primarily using  $^1\text{H}$ ,  $^{13}\text{C}$ -HSQC and  $^1\text{H}$ ,  $^{13}\text{C}$ -HMBC studies. The cross peaks in both the  $^1\text{H}$ ,  $^{13}\text{C}$ -HMBC (Figure 20) and the  $^1\text{H}$ ,  $^{13}\text{C}$ -HSQC (Figure 19) spectra confirm that the signals in the range 169–178 ppm are related to the carbonyl groups of MA units inserted both in-chain and at the end of the branches, according to the previous studies and as certified by the cross peaks in both the  $^1\text{H}$ ,  $^{13}\text{C}$ -HMBC and the  $^1\text{H}$ ,  $^{13}\text{C}$ -HSQC.

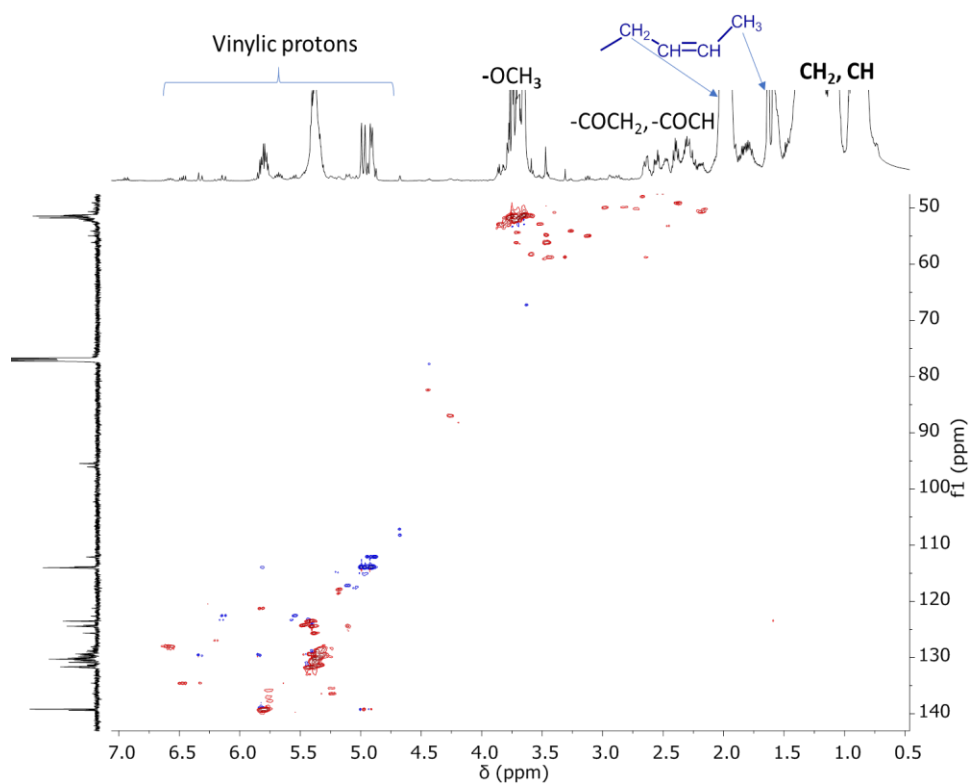


**Figure 19.**  $^1\text{H}$ ,  $^{13}\text{C}$  -HSQC spectrum ( $\text{CDCl}_3$ ,  $T = 298\text{ K}$ ) of sample 14 (Table 2).

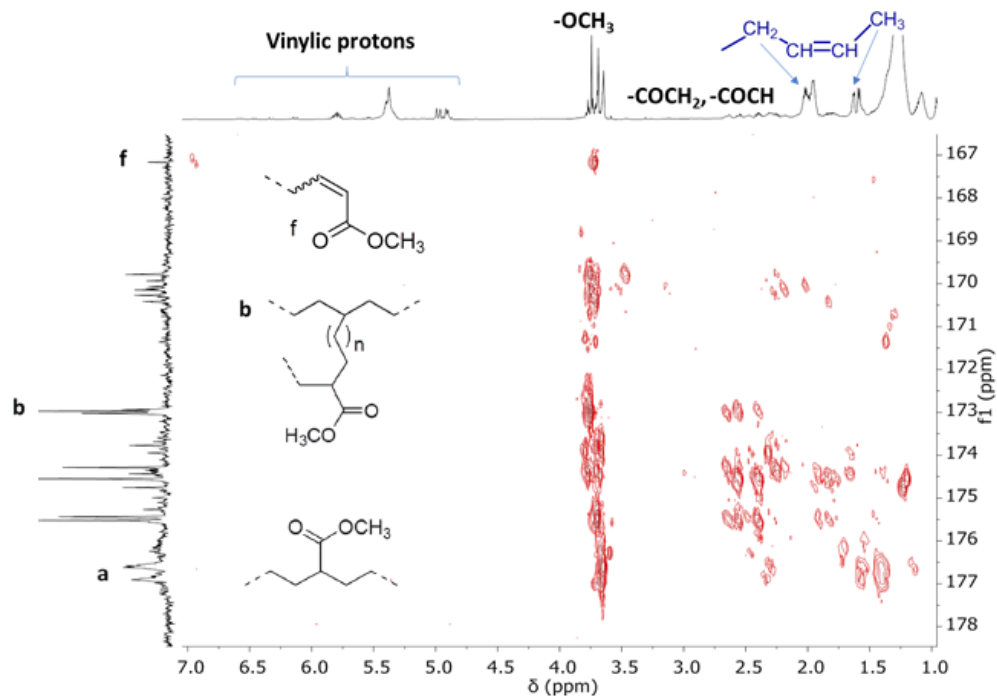


**Figure 20.** Section of  $^1\text{H},^{13}\text{C}$  -HMBC spectrum ( $\text{CDCl}_3$ ,  $T = 298\text{ K}$ ) of sample 14.  $^1\text{H}$  scale: all the required signals;  $^{13}\text{C}$  scale: carbonyl signals only, range 167 -178 ppm.

Furthermore, the carbonyl peak at 174.5 ppm in the  $^1\text{H},^{13}\text{C}$  -HMBC spectrum (Figure 22) indicates two cross peaks with the signals at 12.24 and 12.42 ppm in the  $^1\text{H}$  NMR spectrum. These second ones have a resonance at 96.2 ppm in the  $^{13}\text{C}$  NMR spectrum as well, which has no correlation peak in the  $^1\text{H},^{13}\text{C}$ -HSQC spectrum (Figure 21), implying that it is caused by a quaternary carbon atom.

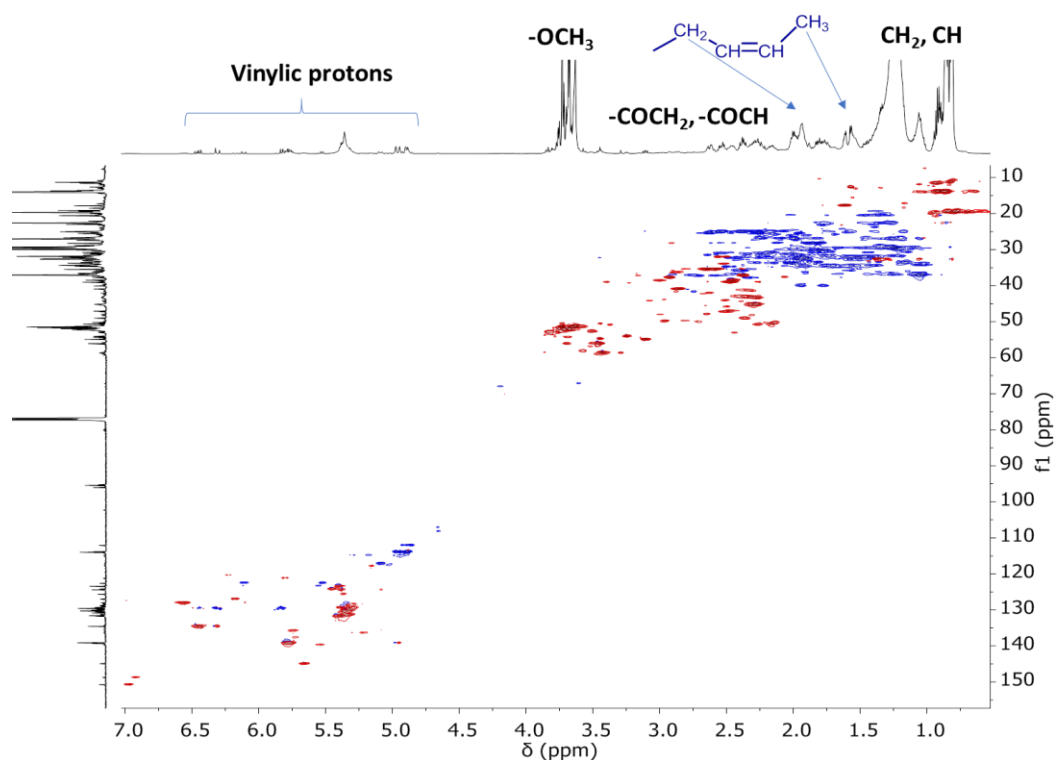


**Figure 21.**  $^1\text{H}, ^{13}\text{C}$ –HSQC spectrum ( $\text{CDCl}_3$ ,  $T = 298\text{ K}$ ) of sample 16 (Table 2).

The signals around 12 ppm are always existing in the  $^1\text{H}$  NMR spectra of all samples, according to a direct observation. These signals are attributable to an acrylic acid moiety (Table 3, fragment g) originating from ester functionality hydrolysis either during the polymerization process or afterward. However, recovering the copolymer by condensing the solvents evaporated from the polymers mixture resulted in the formation of some acrylic acid -OH. This NMR analysis shows that these signals are attributed to an acrylic acid moiety (Table 3, fragment g) obtaining from hydrolysis of the ester functionality occurring during the polymerization process and during the work up as well.

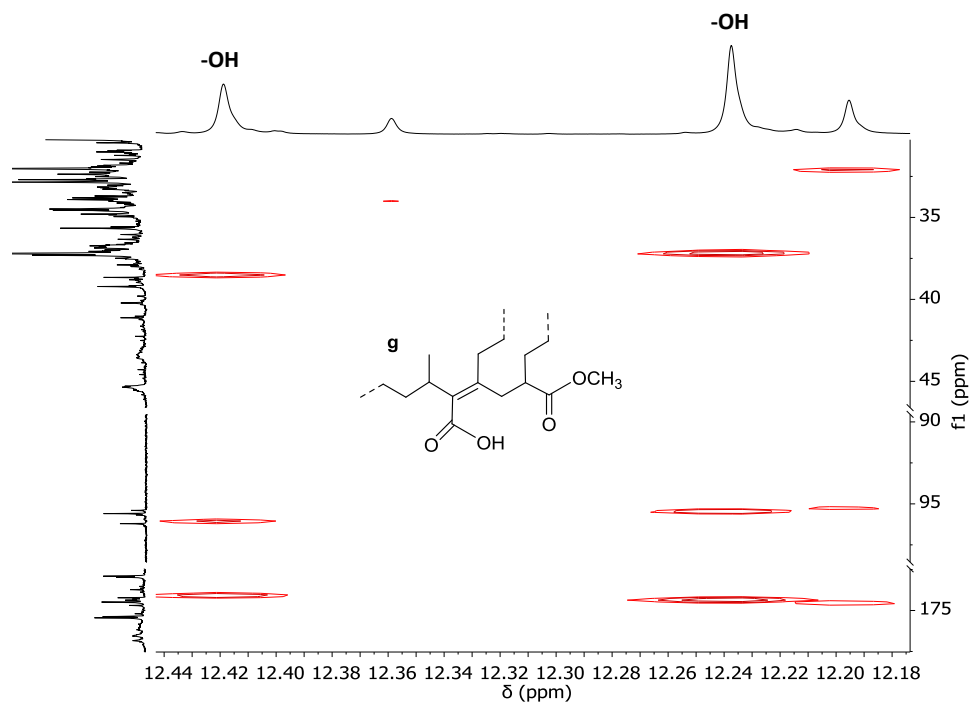


**Figure 22.** Section of  $^1\text{H}, ^{13}\text{C}$  -HMBC spectrum ( $\text{CDCl}_3$ ,  $T = 298 \text{ K}$ ) of sample 16.  $^1\text{H}$  scale: signals at 12.42 and 12.24 ppm;  $^{13}\text{C}$  scale: all the required signals.

Carbonyl group resonances appear at  $^{13}\text{C}$ NMR spectrum at 206.8 and 205.7 ppm and considering other correspondence peaks in the  $^1\text{H}, ^{13}\text{C}$ -HMBC spectrum (Figure 23) show that there is an alternating MA-E-MA sequence (Table 3, fragment c). Similarly, the carbonyl cross peaks at 194.8 ppm shows that there are two isomeric unsaturated moieties related to fragments d and e. (Table 3, Figure 23).

Concerning the small peaks in the 170.4-169.8 ppm range (Figure 16, middle trace), the  $^1\text{H},^{13}\text{C}$  HMBC spectrum indicates cross peaks with the methoxy signal at 3.77 ppm and with the signals of methylenic protons around 2.25 ppm, 1.84 ppm and 2.03 ppm. The attribution of these signals is shown to be for the fragment with two sequential MA units (fragment h, Table 3). This assignment is confirmed by  $^{13}\text{C}$  NMR spectrum of poly(MA) acquired from complex Ni1 (Figure 17).

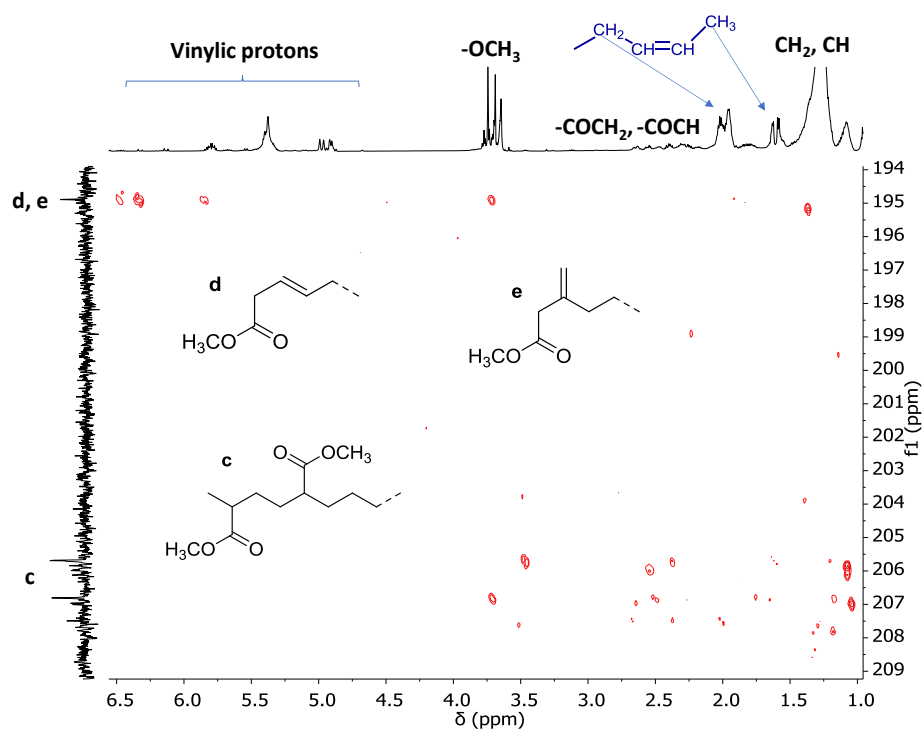


**Figure 23.** Section of  $^1\text{H},^{13}\text{C}$  HMBC spectrum ( $\text{CDCl}_3$ ,  $T = 298\text{ K}$ ) of sample 14.  $^1\text{H}$  scale: all the required signals;  $^{13}\text{C}$  scale: carbonyl signals only, range over 194 ppm.

At last, in accordance with the literature, the carbonyl group that is located at 167.2 ppm was related to the fragment deriving from the  $\beta$ -hydrogen elimination

(BHE) that occurred instantly after the polar monomer was inserted (Figure 20; Table 3, fragment f).

Besides the peaks contributing to the in-chain MA units, the  $^{13}\text{C}$  NMR spectra of Figure 17 upper trace) assign all the resonances discussed for run 14.

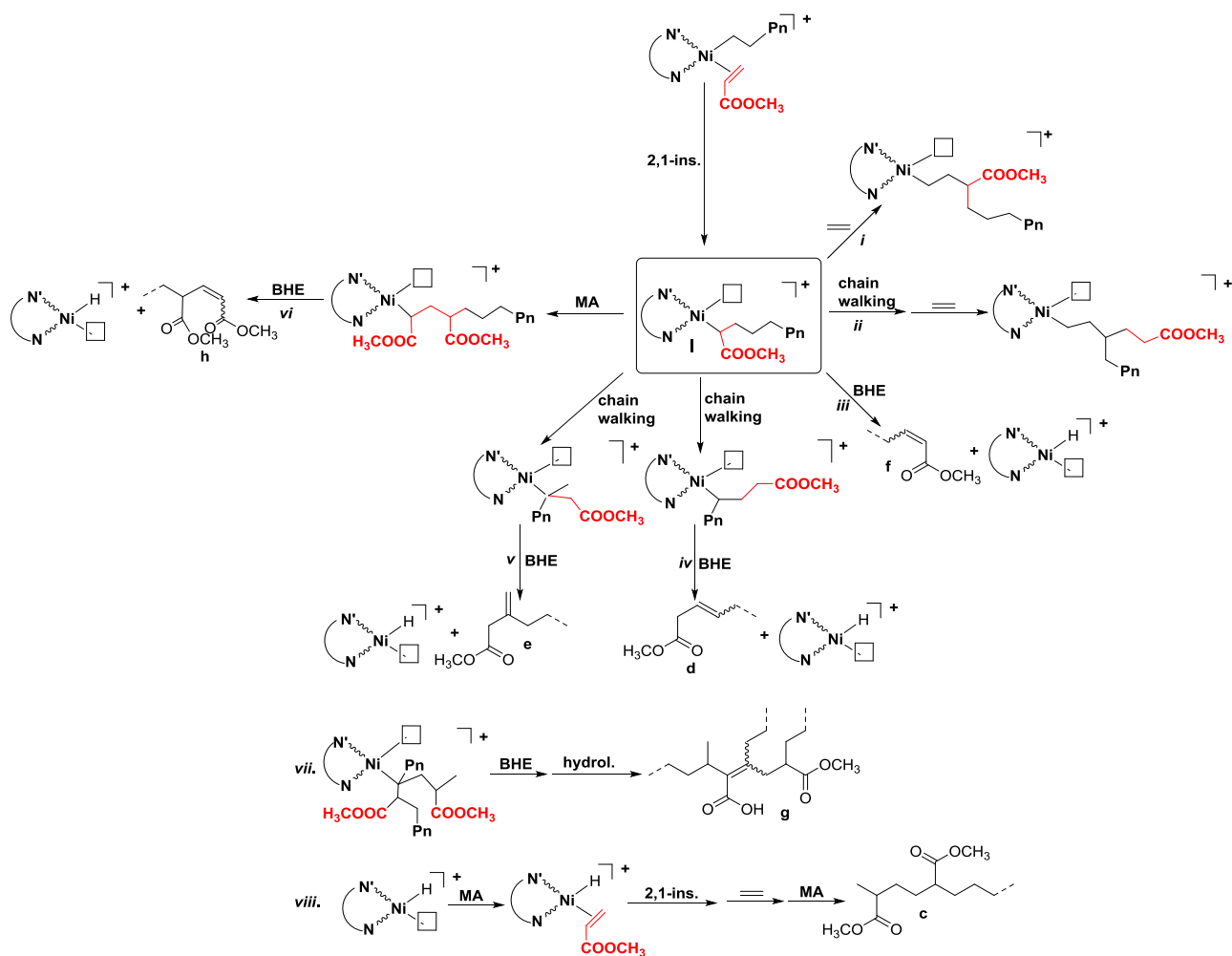
As a result, the MA insertion forms in the three copolymer samples shown in Figure 17 (which are containing of all the different modes of MA insertion reported in Tables 1 and 2) includes from "only in-chain" incorporation in sample 3 to other forms of insertion of MA in sample 6. Table 3 shows the  $^1\text{H}$  and  $^{13}\text{C}$  NMR resonance attributions for all types of MA insertions.

According to the NMR results, the copolymers are hyperbranched macromolecules with MA inserted in various molecular fragments. As a recent study reported, MA can be inserted in-chain even when the chain walking mechanism is active[22]. As a result of the foregoing considerations, the succeeding processes are put forward to describe the various modes of MA incorporation beginning with intermediate I, which is formed by MA insertion into the Ni-alkyl bond via secondary regiochemistry (Scheme 3):

- i. coordination-insertion of several ethylene units leads to fragment a;
- ii. chain walking process leads to fragment b;
- iii. on I  $\beta$ -hydrogen elimination (BHE) can occur leading to fragment f and a Ni-H species;
- iv. fragment d is originated by BHE taking place after MA insertion and chain walking;



- v. similarly, fragment e is the result of BHE taking place as in pathway iv, but on a methyl branch;
- vi. fragment h is the result of BHE taking place after the consecutive insertion of two MA units;
- vii. fragment g is analogous to fragment c and its formation implies the occurrence of BHE during chain walking plus hydrolysis of the ester group.
- viii. fragment c is obtained starting from the Ni-H intermediate, on which coordination-insertion of MA with secondary regiochemistry takes place, followed by coordination-insertion of ethylene and of another molecule of MA leading to the growing of the copolymer chain;



**Scheme 3.** Possible reaction pathways that lead to the detected molecular fragments a-h.

It is challengeable to link the different structures in the different types of MA incorporation with the catalysts and/or reaction conditions. For example, all the samples in Figure 16 have  $^1\text{H}$  NMR spectra were made with the same Ni precatalyst, suggesting that the ligand structure is irrelevant in this case. On the other hand, it appears that the form of activation plays a key role: The NMR

analysis of samples 2 and 6, which were made with the same precatalyst and reaction conditions but a various activation mode, shows that when the activation is done with  $\text{AlMe}_3 / \text{B}(\text{C}_6\text{F}_5)_3 / [\text{Ph}_3\text{C}][\text{B}(\text{C}_6\text{F}_5)_4]$  (as for sample 6) instead of  $\text{AlEt}_2\text{Cl}$  (as for sample 2), the polar monomer is predominantly placed at the end of the branches instead of in-chain. The predominant peak in the  $^1\text{H}$  NMR spectra of the copolymer generated with catalyst **Ni3** after activation with  $\text{AlMe}_3 / \text{B}(\text{C}_6\text{F}_5)_3 / [\text{Ph}_3\text{C}][\text{B}(\text{C}_6\text{F}_5)_4]$  is placed at 3.77 ppm (run 17, Table 2) supports the idea that the activation mode impacts the way the polar monomer is inserted (Figure 24).

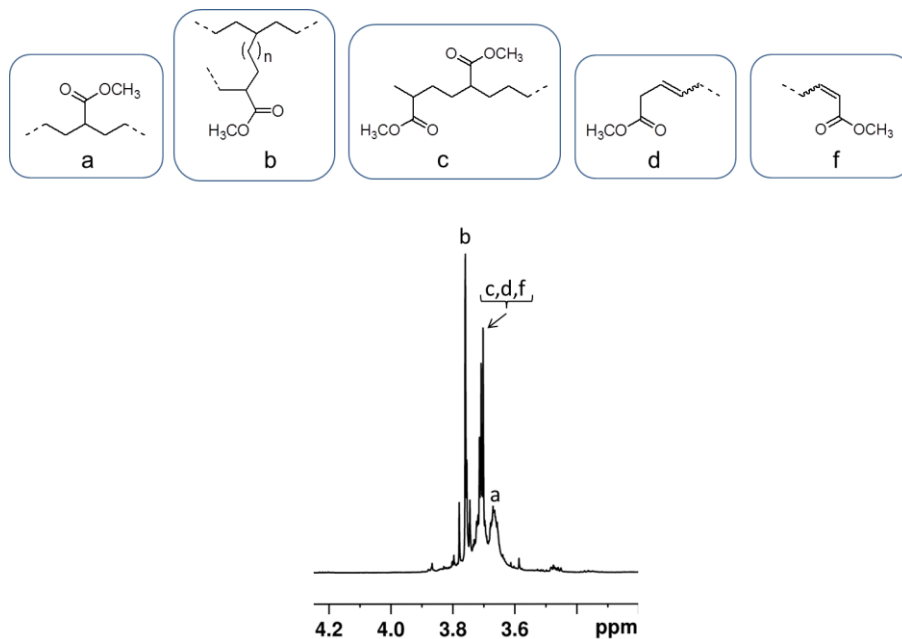


**Figure 24.** Methoxy region of the  $^1\text{H}$  NMR spectrum ( $\text{CDCl}_3$ ,  $T = 298 \text{ K}$ ) of the copolymer sample 17 (Table 2).

The variations in the method of MA insertion in Tables 1 and 2 for samples made with the same Ni precatalyst and  $\text{AlEt}_2\text{Cl}$  cocatalyst is attributed to the various ethylene pressures and the amount of solvent utilized. The most significant difference, however, was the type of solvent employed to solve the Ni complexes, which was o-dichlorobenzene for the Table 1 runs and dichloromethane for the Table 2 runs. Another copolymerization was done with changing the solvent of run 14 for catalyst **Ni3** from dichloromethane to o-dichlorobenzene resulting in a highly in-chain incorporation of MA (run 18, Figure 25 and Figure 26), with the same microstructure with run 3 under 6 atm of ethylene.

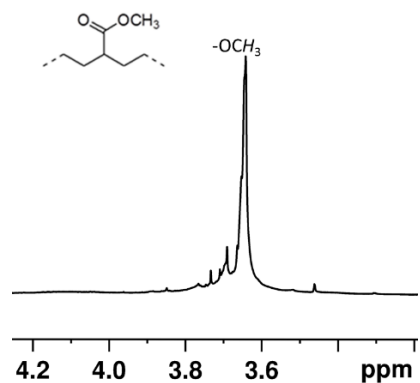


**Figure 25.** Methoxy region of the  $^1\text{H}$  NMR spectrum ( $\text{CDCl}_3$ ,  $T = 298\text{ K}$ ) of the copolymer sample 18 (Table 2).

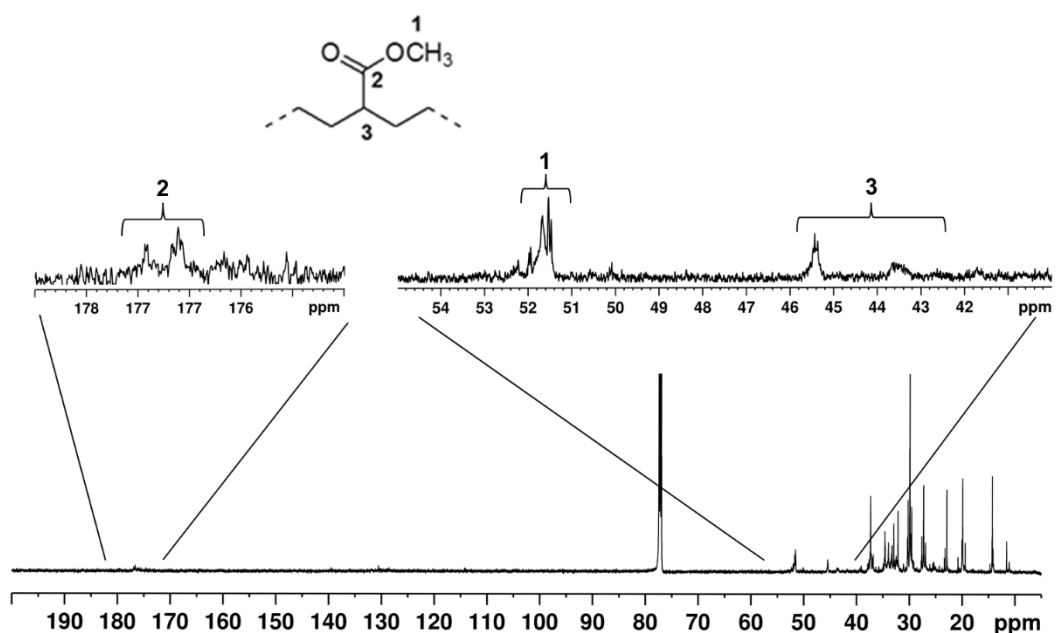


**Figure 26.** <sup>13</sup>C NMR spectrum (CDCl<sub>3</sub>, T = 298 K) of copolymer sample 18 (Table 2) with enlargement of carbonyl, methoxy and methine regions.

Overall, our findings imply that both the activating mode and the solvent used to dissolve the Ni precatalyst influence the mode of MA insertion. When AlEt<sub>2</sub>Cl is used as the cocatalyst and Ni complex is dissolved in *o*-dichlorobenzene, while when we use dichloromethane as the solvent of the Ni catalyst, copolymers with different types of MA insertion are obtained.

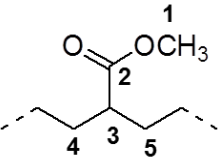
AlMe<sub>3</sub>/ B(C<sub>6</sub>F<sub>5</sub>)<sub>3</sub>/ [Ph<sub>3</sub>C][B(C<sub>6</sub>F<sub>5</sub>)<sub>4</sub>] activation also produces copolymers with different types of MA incorporation. Our findings also reveal that activation with AlEt<sub>2</sub>Cl in dichloromethane or AlMe<sub>3</sub>/ B(C<sub>6</sub>F<sub>5</sub>)<sub>3</sub>/ [Ph<sub>3</sub>C][B(C<sub>6</sub>F<sub>5</sub>)<sub>4</sub>] obtains similar result, which are incline to produce β-hydride elimination reactions after

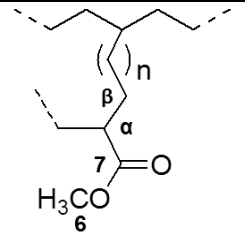
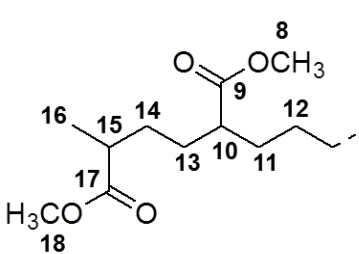
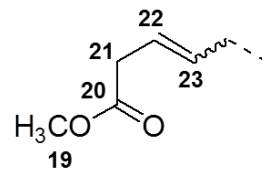
the acrylate insertion, resulting in fragments d, e, and f (Table 3), as well as the Ni-H intermediate capable of inserting a molecule of MA (Table 3).

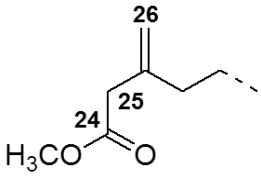
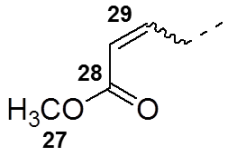
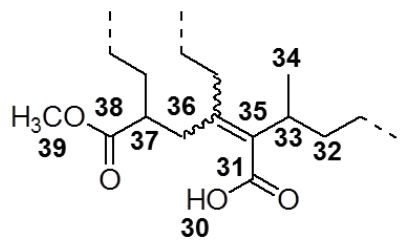
A recent study have reported the effects of the solvent on the microstructure of ethylene-methyl acrylate copolymers for  $\alpha$ -diimine Pd catalysts [23]. When copolymerization is performed in dichloromethane rather than trifluoroethanol, incorporation seem to be with a less selective enchainment.

Brookhart studied the influence of several activating agents on productivity in the Ni-catalyzed copolymerization of ethylene with vinyltrialkoxysilanes, but found no differences in the copolymer microstructure [17, 18].

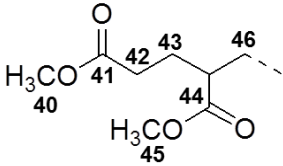
**Table 3.** Molecular fragments containing MA in the synthesized E-MA copolymers with the corresponding  $^1\text{H}$  and  $^{13}\text{C}$  NMR resonance assignments<sup>a</sup>.

	Fragments	NMR Shifts		
		n	$^1\text{H}$	$^{13}\text{C}$
<b>a</b>		<b>1</b>	3.67	51.5
		<b>2</b>	-	176.7, 176.4
		<b>3</b>	2.33	45.4
		<b>4</b>	1.58	34.6
		<b>5</b>	1.40	32.2
<b>b</b>		<b>6</b>	3.77	51.6
		<b>7</b>	-	172.9
		<b><math>\alpha</math></b>	2.32	43.4

		<b>β</b>	1.65	24.5
<b>c</b>		<b>8</b>	3.47	55.2
		<b>9</b>	-	205.7
		<b>10</b>	2.38	49.1
		<b>11</b>	2.54	25.0
		<b>12</b>	1.08	27.0
		<b>13</b>	1.17	36.1
		<b>14</b>	1.76	34.5
		<b>15</b>	2.50	39.2
		<b>16</b>	1.04	14.1
		<b>17</b>	-	206.8
<b>d</b>		<b>19</b>	3.70	51.6
		<b>20</b>	-	194.8
		<b>21</b>	1.38	32.7
		<b>22</b>	6.50/5.86	134.7/139.3
		<b>23</b>	6.50/5.86	134.7/139.3
<b>e</b>		<b>24</b>	-	194.8
		<b>25</b>	1.38	32.7

		<b>26</b>	6.34	129.8
<i>f</i>		<b>27</b>	3.73	52.2
		<b>28</b>	-	167.2
		<b>29</b>	6.9/7.0	148.9
<i>g</i>		<b>30</b>	12.24	-
		<b>31</b>	-	174.5
		<b>32</b>	2.54/2.38	25.2
		<b>33</b>	2.37	37.2
		<b>34</b>	1.17	17.3
		<b>35</b>	-	95.6
		<b>36</b>	2.26/2.63	25.7
		<b>37</b>	2.37	37.2
		<b>38</b>	-	175.4
		<b>39</b>	3.70	51.9
<i>h</i>		<b>40</b>	3.77	51.6
		<b>41</b>	-	169.8/170.4
		<b>42</b>	2.25	25.7

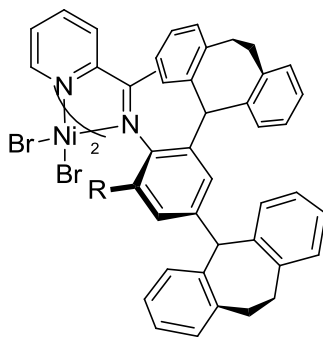


	<b>43</b>	2.03	27.2
	<b>44</b>	-	169.8/170.4
	<b>45</b>	3.77	51.6
	<b>46</b>	1.84	30.5

<sup>a</sup> NMR spectra recorded in CDCl<sub>3</sub> at T = 298 K.

## 2.2. Copolymerization of Ethylene and Methyl Acrylate by Dibenzocycloheptyl-substituted Aryliminopyridyl Ni(II) catalysts

Nickel bromide precatalysts carrying 2-((arylimino)ethyl)pyridine derivatives containing N-2,4-bis(dibenzocycloheptyl) owing different properties sterically and electronically (Figure 27) were employed in copolymerization reactions of ethylene with methyl acrylate. Firstly, **Ni5-Ni9** were assessed under 6 atm of ethylene by using 6  $\mu\text{mol}$  of the Ni precatalyst activated with 500 equiv of  $\text{AlEt}_2\text{Cl}$  and  $[\text{MA}] = 0.1 \text{ M}$  at  $30 \text{ }^\circ\text{C}$  for 18 h.



No.5 R = Me,  
No.6 R = Et,  
No.7 R = iPr,  
No.8 R = Cl,  
No.9 R = F,

**Figure 27.** Dibenzocycloheptyl-substituted aryliminopyridyl Ni(II) complexes **5-9**.

Results are reported in the Table 4. After quenching the reaction solution with acidified methanol in all runs, a solid copolymer was obtained. Among the first three catalysts which are electron-donating, catalyst 6 with 1.5 g copolymer and 1% MA incorporation is the most active catalyst. Subsequently, catalyst 7 with 1 g copolymer and 2% MA incorporation comes to be the second active catalyst.

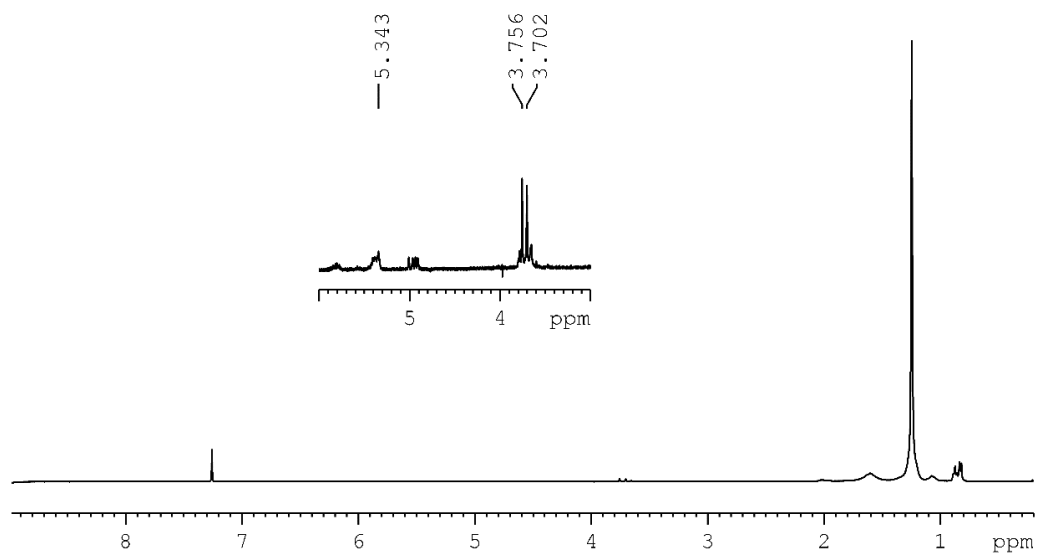
Catalyst 1 had the least activity with 0.2 g copolymer and 0.5% MA incorporation (Table 4). The activity of the other two complexes 8 and 9, which contains electron-withdrawing substituents, is reduced.

**Table 4.** Ethylene-Methyl Acrylate Copolymerizations by Complexes **5–9** under 6 atm of Ethylene.

Entry	Complex	Yield (g)	MA <sup>b</sup> (Mol%)	M <sub>n</sub> <sup>c</sup>	N <sup>d</sup> branches
1	<b>5</b>	0.2	0.5	3428	47
2	<b>6</b>	1.5	1	3218	63
3	<b>7</b>	1	2	3981	55
4	<b>8</b>	0.07	1.7	2977	64
5	<b>9</b>	0.04	9.3	3202	41

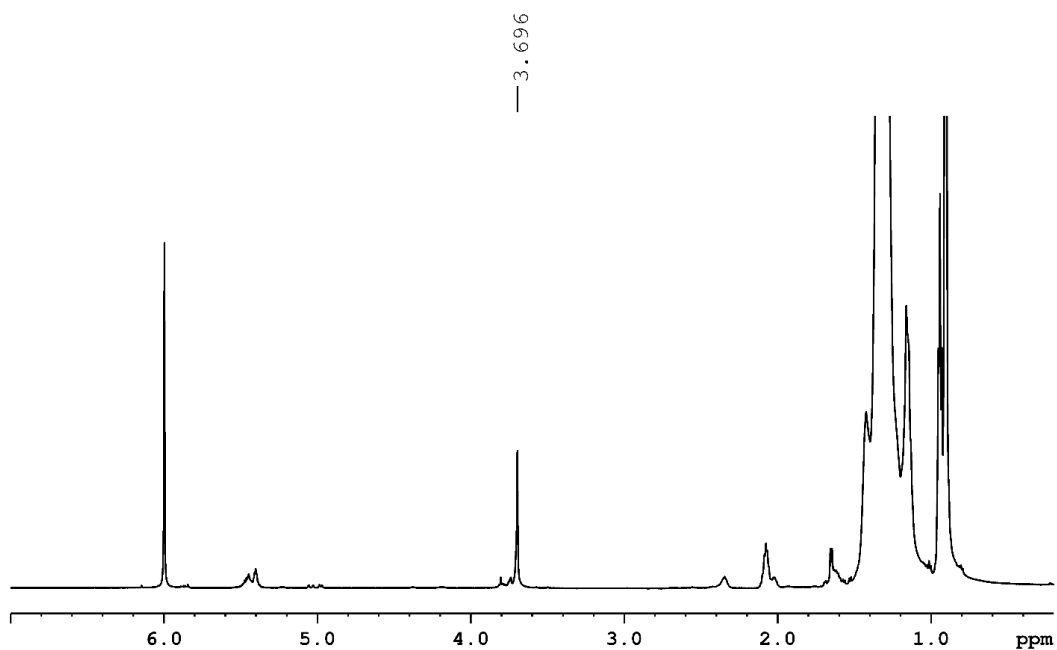
<sup>a</sup>Polymerization conditions: Ni catalyst = 6  $\mu$ mol dissolved in 2 mL of o-dichlorobenzene; cocatalyst = AlEt<sub>2</sub>Cl (5 mmol); solvent = 100 mL of toluene; MA = 10 mmol; T = 30 °C; P<sub>E</sub> = 6 atm; time 18 h. <sup>b</sup>Incorporation of MA in the copolymer determined by <sup>1</sup>H NMR. <sup>c,d</sup>Determined by <sup>1</sup>H NMR.

The copolymer from entry 1 was analyzed by <sup>1</sup>H NMR in CDCl<sub>3</sub> at room temperature (see Figure 28). There are three peaks in the methoxy region. The main peak is related to end-chain incorporation.



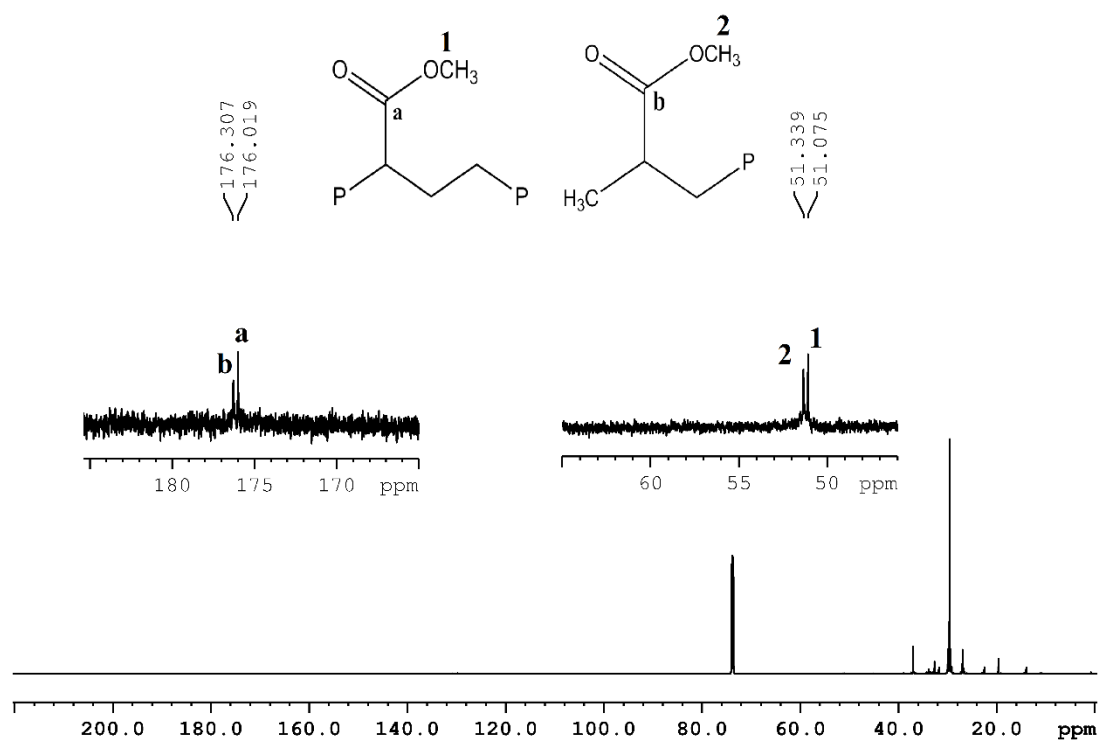
**Figure 28.**  $^1\text{H}$  NMR spectra ( $\text{C}_6\text{D}_4\text{Cl}_2$ ,  $T = 298\text{ K}$ ) of the copolymer sample of entry 1.

The copolymer obtained from entry 2 was analyzed by  $^1\text{H}$  and  $^{13}\text{C}$  NMR in  $\text{C}_6\text{D}_4\text{Cl}_2$  at  $80^\circ\text{C}$  showing that there is only one main peak at methoxy protons of MA units located at 3.69 ppm which is related to the in-chain incorporation of MA units (Figure 29).



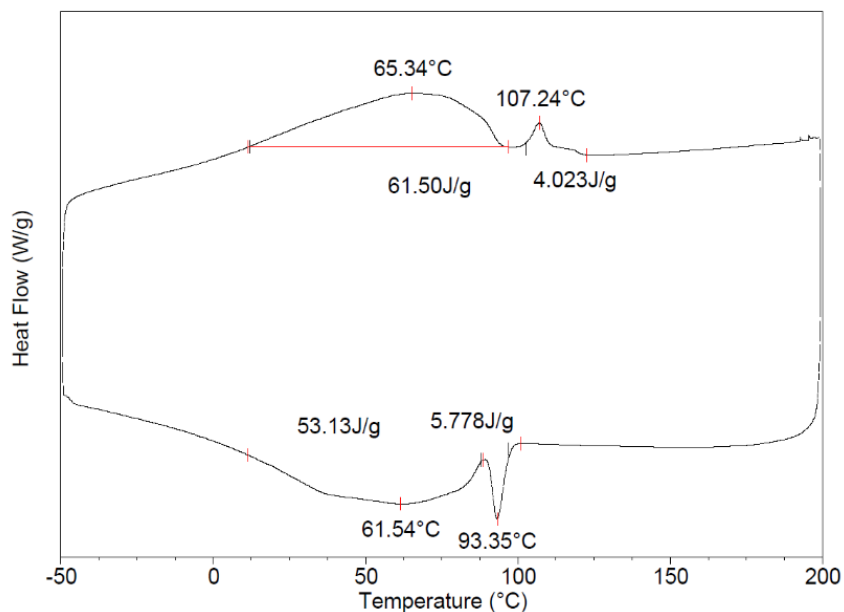
**Figure 29.**  $^1\text{H}$  NMR spectrum ( $\text{C}_6\text{D}_4\text{Cl}_2$ ,  $T = 353\text{ K}$ ) of the copolymer sample of entry 2.

The existence of peaks at 176.01, 176.30 ppm in the carbonyl region of a  $^{13}\text{C}$  NMR of the same sample verified that according to the literature [24], these peaks are attributed to MA units inserted in-chain (fragment a, fragment b, table 3) and resonances at  $\delta 51.07$  and 51.34 are related to the methoxy group respectively (Figure 30).



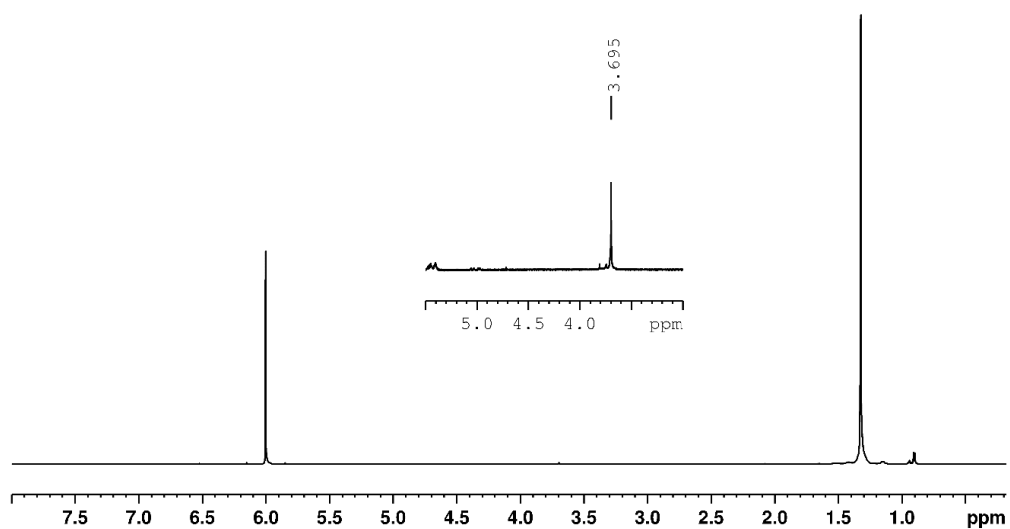
**Figure 30.**  $^{13}\text{C}$  NMR spectrum ( $\text{C}_6\text{D}_4\text{Cl}_2$ ,  $T = 353\text{ K}$ ) of the copolymer sample of entry 2.

The copolymer sample had a significant broad melting transition centered at  $65^\circ\text{C}$  and a minor melting peak at  $107^\circ\text{C}$ , according to DSC analysis (Figure 31).

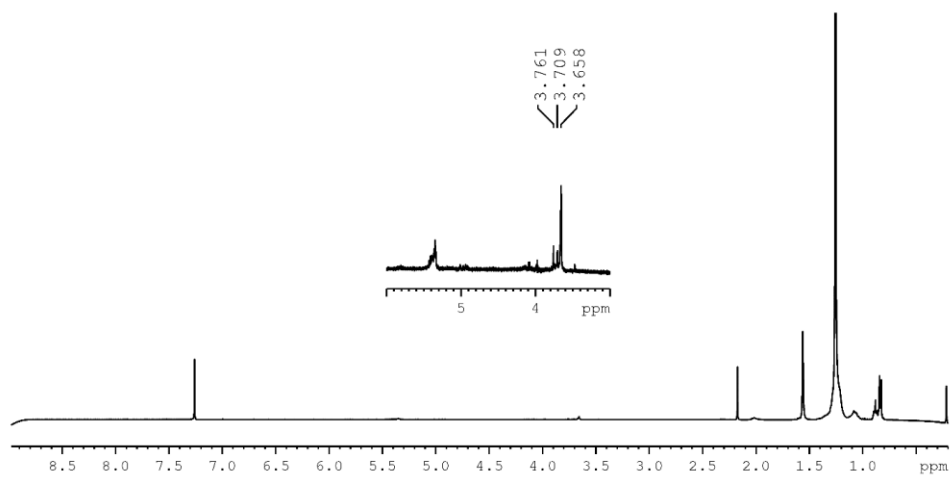


**Figure 31.** DSC from the copolymer of entry 2 (Raw polymer).

In a Kumagawa extractor, the material was fractionated with boiling pentane, and the soluble and insoluble fractions were separated. Both soluble and insoluble parts were analyzed by  $^1\text{H}$  NMR and DSC. The soluble part (70%) and the insoluble part (30%) were analyzed by  $^1\text{H}$  NMR. The soluble part was a copolymer with 0.7% MA incorporation, while the insoluble part was a copolymer with 1.4% MA incorporation. Both parts were analyzed by  $^1\text{H}$  NMR. The  $^1\text{H}$  NMR spectrum of the insoluble part indicated only in-chain incorporation of methyl acrylate (Figure 32) and the  $^1\text{H}$  NMR spectrum of the soluble part contains mainly in-chain incorporation and two minor peaks.



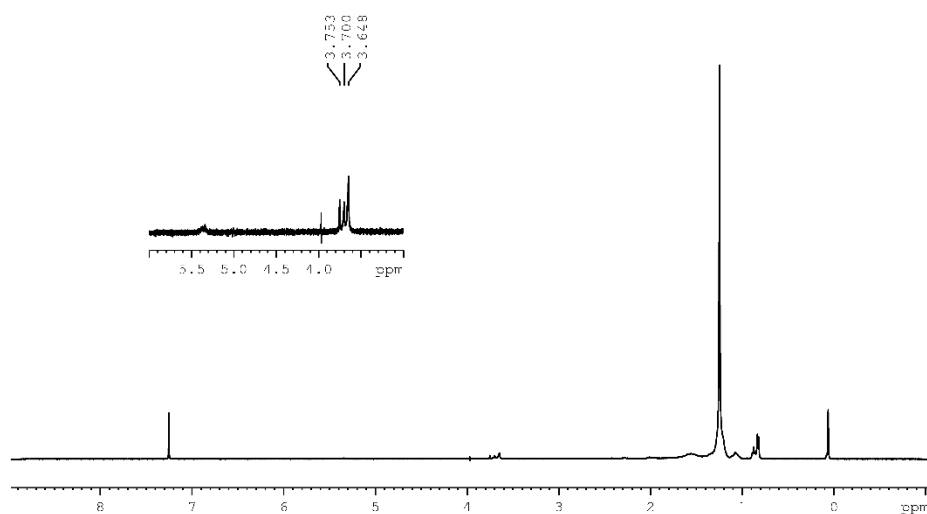
**Figure 32.**  $^1\text{H}$  NMR spectra ( $\text{C}_6\text{D}_4\text{Cl}_2$ ,  $T = 353\text{ K}$ ) of the pentane-insoluble fraction of the copolymer sample of entry 2.



**Figure 33.**  $^1\text{H}$  NMR spectra ( $\text{CDCl}_3$ ,  $T = 298\text{ K}$ ) of the pentane-soluble fraction of the copolymer sample of entry 2.

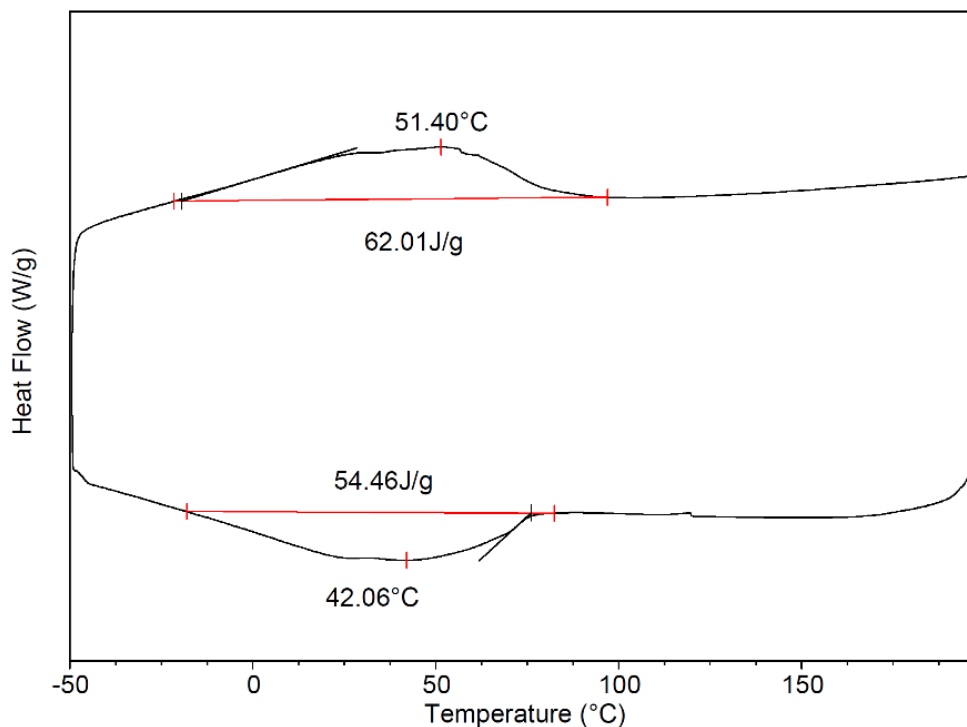


Copolymer obtained from sample 7 was also analyzed by  $^1\text{H}$  NMR spectrum indicated three peaks in methoxy region are related to the different modes of MA incorporation including both in-chain and end-of-chain MA incorporation (Figure 34).



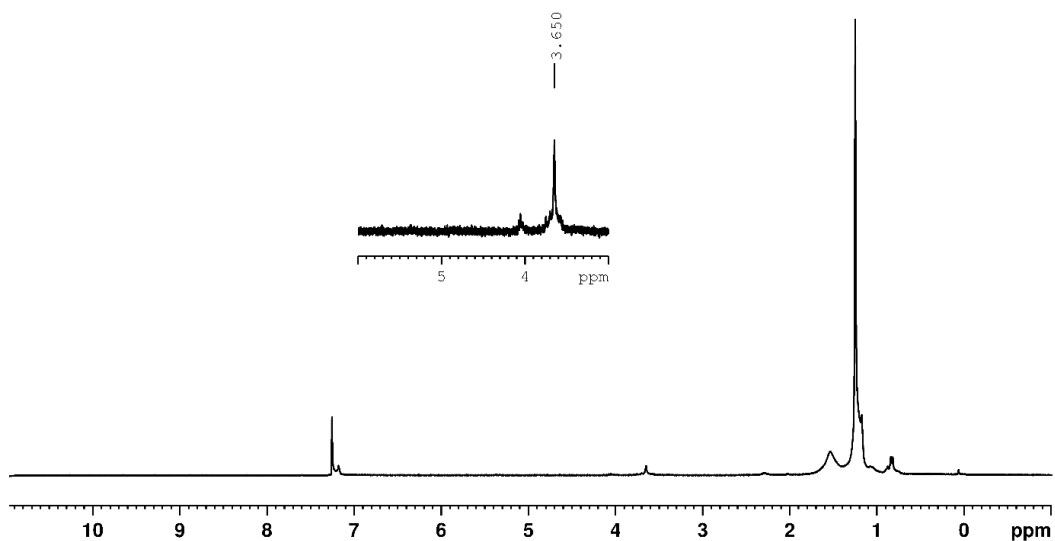
**Figure 34.**  $^1\text{H}$  NMR spectra ( $\text{C}_6\text{D}_4\text{Cl}_2$ ,  $T = 298\text{ K}$ ) of the copolymer sample of entry 3.

Figure 35 shows DSC analysis for copolymer obtained from run 3 showing a broad melting transition centered at  $51.40\text{ }^\circ\text{C}$ .



**Figure 35.** DSC from the copolymer of entry 3 (Raw polymer).

As with entry 3, the copolymer sample was extracted with boiling pentane and the soluble (70%) and insoluble components were examined using  $^1\text{H}$  NMR. The soluble component was a copolymer with a lower molecular weight and an MA incorporation of 0.7%, whereas the insoluble component was a copolymer with a higher molecular weight and an MA incorporation of 1.6%. Both components were characterized using  $^1\text{H}$  and  $^{13}\text{C}$  NMR spectroscopy. The  $^1\text{H}$  NMR spectra of the insoluble component suggested that methyl acrylate was predominantly incorporated in-chain (Figure 36).



**Figure 36.**  $^1\text{H}$  NMR spectrum ( $\text{CDCl}_3$ ,  $T = 298 \text{ K}$ ) of the pentane-insoluble fraction of the copolymer sample of entry 3.

The  $^1\text{H}$  NMR spectrum of the insoluble component revealed three peaks in the methoxy region in which methyl acrylate was mainly incorporated in-chain (Figure 37).

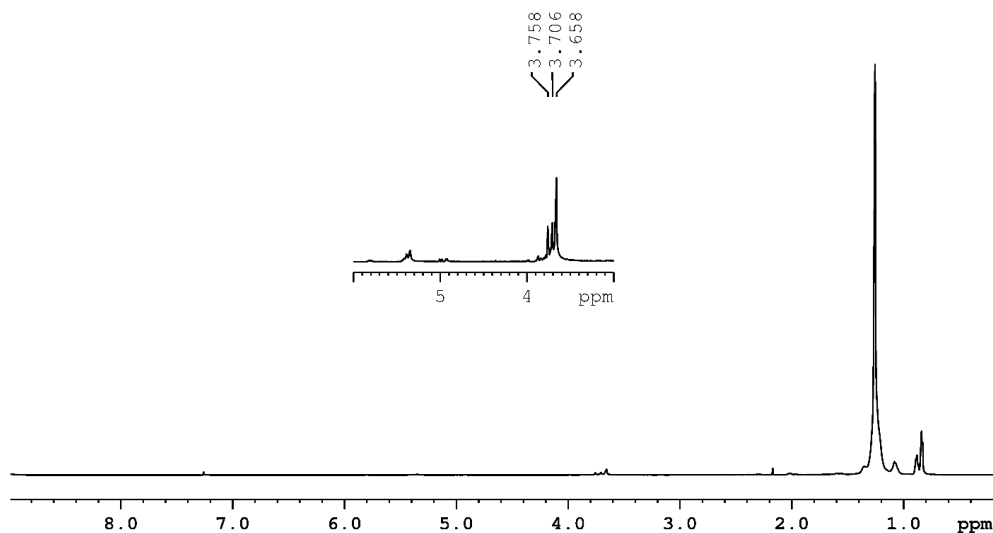


**Figure 37.**  $^1\text{H}$  NMR spectra ( $\text{CDCl}_3$ ,  $T = 298\text{ K}$ ) of the pentane-soluble fraction of the copolymer sample of entry 3.

The  $^{13}\text{C}$  NMR spectrum of soluble part of entry 3 indicates that copolymer produced by complex 3 is less selective for in-chain MA insertion than complex 6. As is shown in Figure 38 in carbonyl region of the spectrum, different resonances are found, 176.7, 175.7, 174.8, 173.2 ppm indicating that in addition to the peaks which are inserted in-chain, 176.7 ppm, there are other three peaks related to other types of incorporations as previously reported in the first chapter (fragment b, c, g, table 3) [20]. Resonances at  $\delta$  51.6, 51.7, 52.02, 52.2, 52.4 are observed for the methoxy group and at 45.5 ppm for the methine carbons of the MA units.

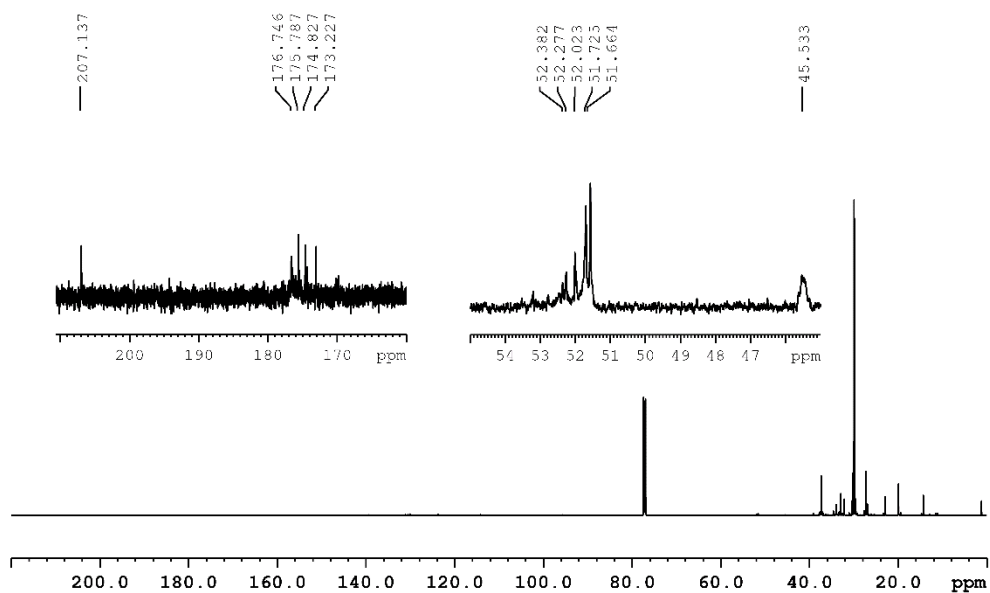


**Figure 38.**  $^{13}\text{C}$  NMR spectrum ( $\text{CDCl}_3$ ,  $T = 353\text{ K}$ ) of the copolymer sample of entry 3.

Following that, complexes 1 and 2 were evaluated in E-MA copolymerization of ethylene and MA at higher ethylene pressures, i.e. 10, 20, 40 atm. In all runs, solid polymers precipitated in acidified methanol. As anticipated, as the pressure of ethylene is increased, the amount of MA inserted reduces and the amount of copolymer produced increases (Table 5).

The  $^1\text{H}$  NMR spectrum of the copolymer produced by catalyst 6 at 30 atm of ethylene (entry 7) exhibits three peaks in the methoxy region, in contrast to the result obtained at 6 atm (Figure 39), showing that various ways of MA insertion are feasible. The mechanism of MA insertion was noticed to be dependent on the reaction conditions for catalysts based on iminopyridyl Ni(II) complexes. After fractionating the copolymer of entry 7 with boiling pentane in a Kumagawa

extractor, the soluble (30%) and insoluble (70%) parts were characterized by  $^1\text{H}$  NMR. The spectrum of the insoluble part reveals that the major methoxy resonance is due to in-chain MA incorporation (1.1 % MA incorporation) (Figure 40).

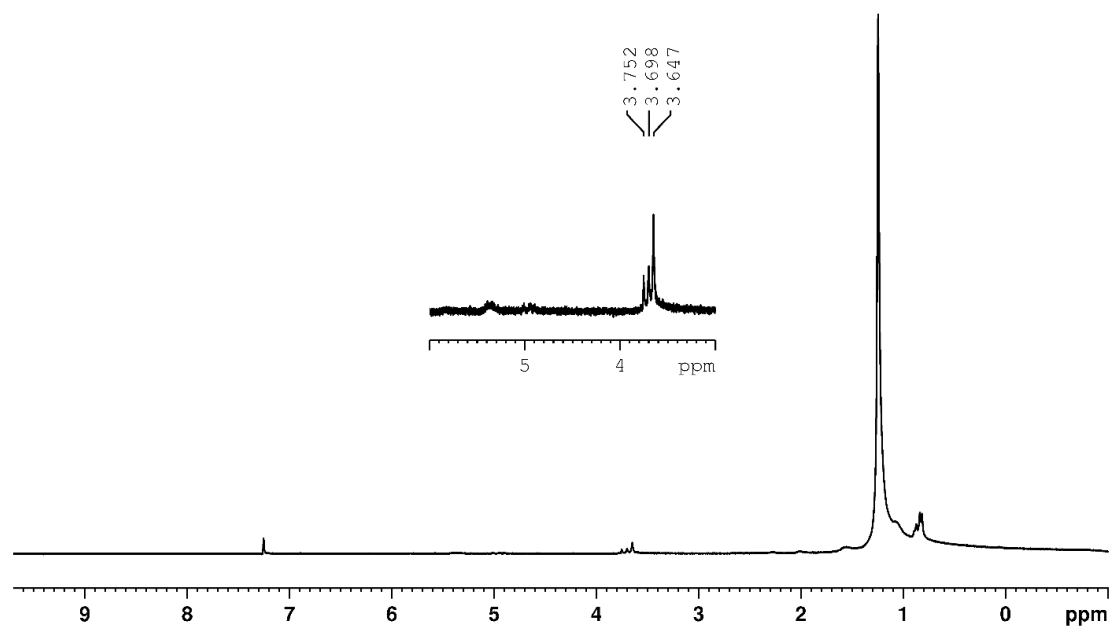


**Figure 39.**  $^1\text{H}$  NMR spectra ( $\text{CDCl}_3$ ,  $T = 298\text{ K}$ ) of the copolymer sample of entry 7.

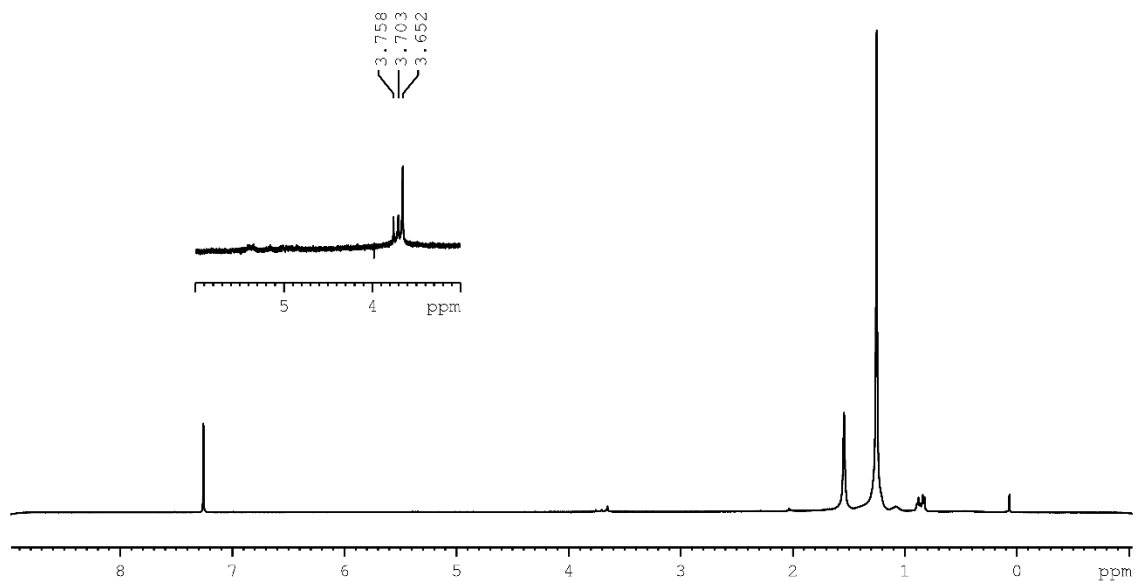


**Figure 40.** <sup>1</sup>H NMR spectra (CDCl<sub>3</sub>, T = 298 K) of the pentane-insoluble fraction of the copolymer sample of entry 7.

The soluble part was analyzed by <sup>1</sup>H NMR showing three peaks with majority of end-chain incorporation of MA insertion with less molecular weight than insoluble part (Figure 41).

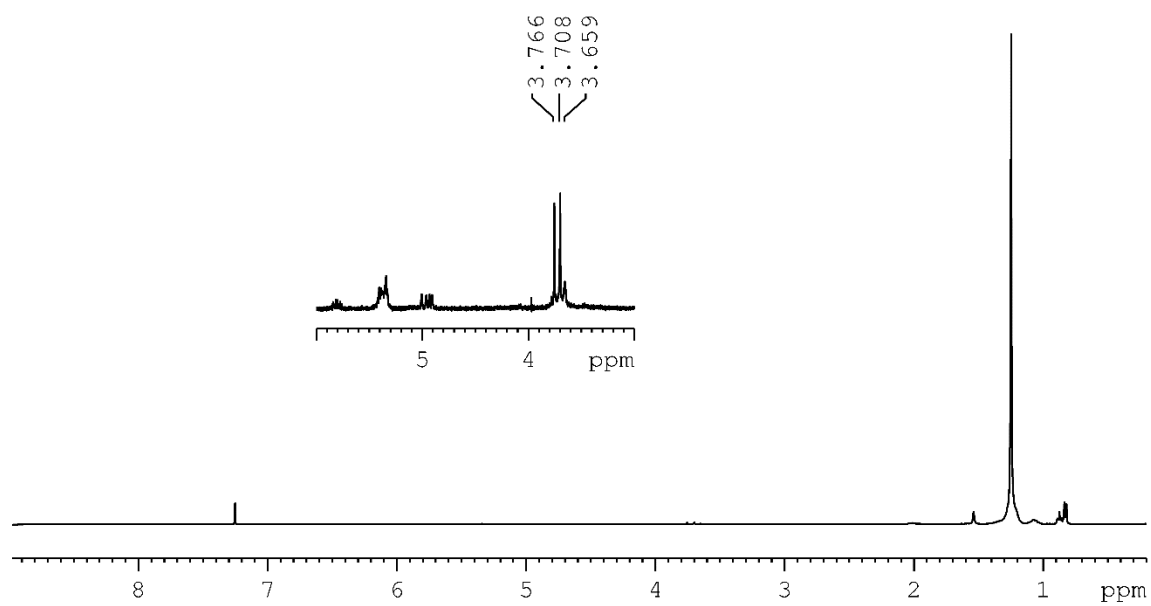


**Figure 41.**  $^1\text{H}$  NMR spectra ( $\text{CDCl}_3$ ,  $T = 298\text{ K}$ ) of the pentane-soluble fraction of the copolymer sample of entry 7.



**Table 5.** Ethylene-Methyl Acrylate Copolymerization by Complexes 1 and 2 under Higher Ethylene Pressures.

Entry	Complex	P (atm)	t (h)	Yield (g)	MA <sup>b</sup> (mol%)	M <sub>n</sub> <sup>c</sup>	N <sup>d</sup> branch es
6	<b>6</b>	30	18	1.0	0.4	2385	36
7	<b>5</b>	30	18	1.3	0.4	1664	31
8	<b>6</b>	10	18	0.4	0.8	2335	45
9	<b>6</b>	40	18	1.2	0.3	1497	26
10	<b>5</b>	10	18	0.4	0.7	4378	46
11	<b>5</b>	20	18	0.7	0.9	1591	29
12	<b>5</b>	40	18	0.9	0.4	2062	31

<sup>a</sup>Polymerization conditions: Ni catalyst = 6  $\mu$ mol dissolved in 2 mL of o-dichlorobenzene; cocatalyst = AlEt<sub>2</sub>Cl (5 mmol); MA = 10 mmol; solvent = 100 mL of toluene; T = 30 °C.

<sup>b</sup>Incorporation of MA in the copolymer determined by <sup>1</sup>H NMR. <sup>c,d</sup>Determined by <sup>1</sup>H NMR.

The <sup>1</sup>H NMR of the sample produced by complex **5** under 30 atm of ethylene (entry 8) also shows three resonances in the methoxy region, although in this case the main resonance is that attributed to in-chain incorporation of MA (Figure 42).

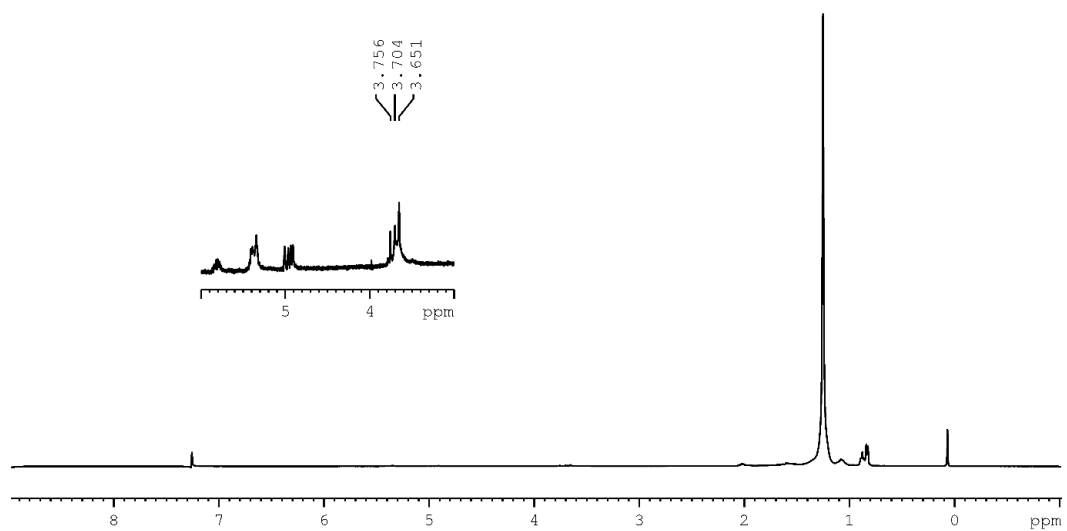


**Figure 42.**  $^1\text{H}$  NMR spectra ( $\text{CDCl}_3$ ,  $T = 298\text{ K}$ ) of the copolymer sample of entry 8.

### 2.3. Iminopyridine Ni(II) catalysts affording either oily hyperbranched oligoethylenes or crystalline polyethylenes depending on the reaction conditions: possible role of in situ catalyst structure modifications

We have also investigated complex 1 and some related Ni(II) complexes in ethylene polymerization also at subambient temperature and high pressures, resulting in the production of solid polymers, in some cases consisting of fractions with different crystallinities, either as the only product or together with a methanol-soluble oily fraction.

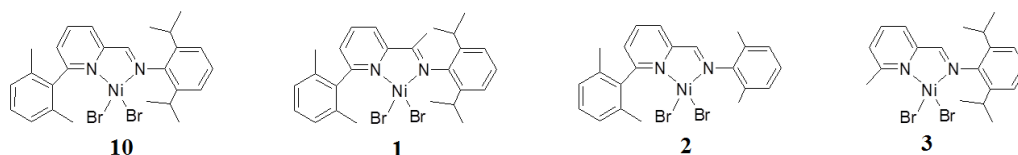


**Figure 43.** Iminopyridine Ni complexes **1-3,10**.

Catalyst 10 was investigated following activation with 200 equiv of  $\text{AlEt}_2\text{Cl}$  at  $0^\circ\text{C}$  under 50 atm pressure of ethylene (run 1, Table 6): under these conditions, besides the normal oily fraction obtained from the reaction solution, a solid polymer was formed as the predominant. The  $^1\text{H}$  and  $^{13}\text{C}$  NMR analysis of both fractions (Figure 44, Figure 45) revealed that the liquid part is a hyperbranched polyethylene analogous to those previously described [25], whereas the first is a moderately branched polyethylene with a high proportion of methyl branches ( $N_{\text{Me}} = 84\%$ ).

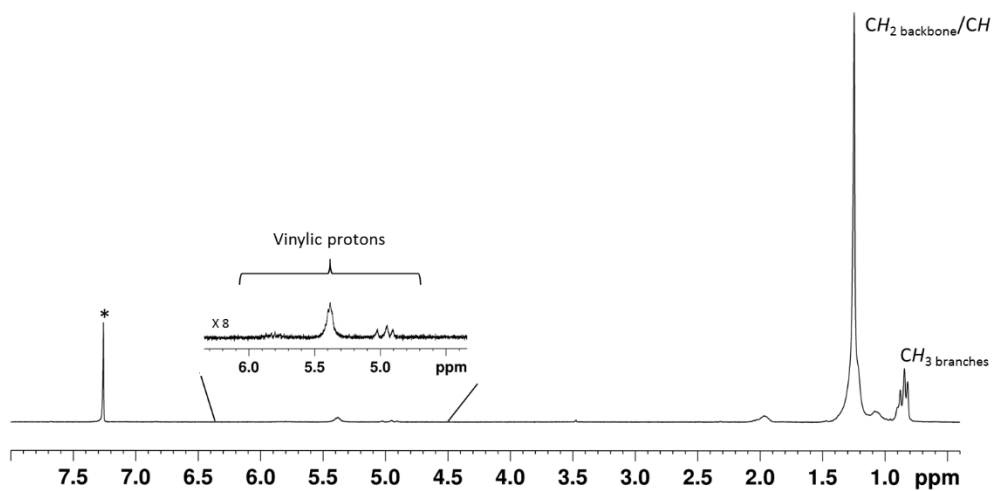


**Figure 44.**  $^1\text{H}$  NMR ( $\text{CDCl}_3$ ,  $T = 298\text{ K}$ ) spectrum of oily fraction obtained in run 1, Table 6.

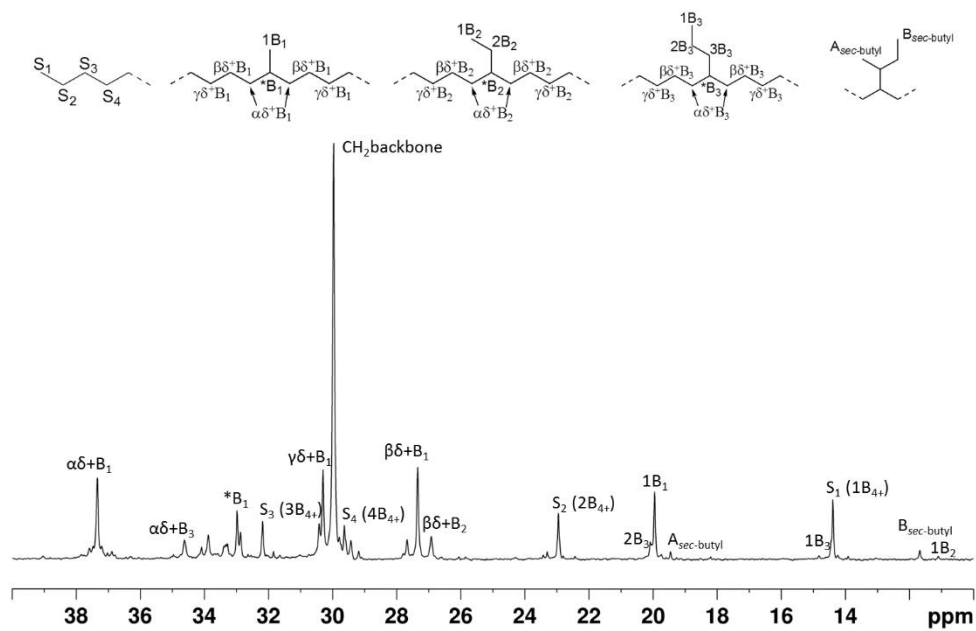


**Figure 45.**  $^{13}\text{C}$  NMR ( $\text{CDCl}_3$ ,  $T = 298\text{ K}$ ) spectrum of oily fraction obtained in run 1, Table 6.

Following that, similar compounds with various substituents at the pyridino and imino moieties (complexes 1-3, Figure 43) were investigated.

Catalysts 1-3 were initially evaluated in the homopolymerization of ethylene following activation with  $\text{AlEt}_2\text{Cl}$  (200 equiv) at 40 °C and 6 atm monomer pressure (Table 6, runs 1-4): all complexes produced hyperbranched low molecular weight polyethylene oils that were soluble in methanol, corresponding to those obtained by catalyst 10 [25].

The  $^1\text{H}$  and  $^{13}\text{C}$  NMR characterization of the polymer samples were investigated. As observed for catalyst 10, different amounts of low molecular weight polyethylene oils were produced at increased catalyst and monomer quantities and for longer reaction durations, indicating that the catalysts are stable at these environments (runs 5-8). Catalyst 1, including a ketimino ligand, produced polyethylene with a higher molecular weight than the described earlier aldimino complex 1 [25].

Complex 1 was subsequently investigated under 50 atm of ethylene pressure at 0 °C (run 9, Table 6): resulting in only a solid polymer and no oily product was extracted from the reaction solution. NMR analysis showed a moderately branched polyethylene (5 % branches), while DSC revealed extremely broad melting endotherms located around 32 and 71 °C and vastly broad crystallization exotherms located around 57 and 24 °C.

**Table 6.** Ethylene polymerizations by complexes **1-3,10**

Run	Complex	T (°C)	P <sub>(ethylene)</sub> (atm)	time (h)	Yield (g)	Activity <sup>a</sup>	M <sub>n</sub> <sup>a</sup> (kDa)	PDI <sup>c</sup>	% branches <sup>b</sup>
1 <sup>e</sup>	10	0	50	4	1.00 <sup>f</sup> +	25	0.9	3.1	6.2
					2.80 <sup>e,g</sup>	70	4.5	2.6	3.2
2 <sup>e</sup>	1	40	6	4	0.96 <sup>f</sup>	24	2.0	1.3	7.4
3 <sup>e</sup>	2	40	6	4	1.07 <sup>f</sup>	27	0.73	1.3	10.5
4 <sup>e</sup>	3	40	6	4	1.4 <sup>f</sup>	35	0.35	1.2	9.0
5 <sup>h</sup>	1	40	10	4	4.58 <sup>f</sup>	114	3.6	1.4	7.3
6 <sup>h</sup>	1	40	30	20	11.0 <sup>f</sup>	55	3.10	1.4	8.2
7 <sup>h</sup>	2	40	10	4	5.21 <sup>f</sup>	130	0.58	1.3	8.9
8 <sup>h</sup>	3	40	10	4	4.15 <sup>f</sup>	104	0.30	1.1	8.8
9 <sup>e</sup>	1	0	50	4	0.91 <sup>e,g</sup>	23	5.20	3.2	5.0

<sup>a</sup> Activity in kg mol<sub>[Ni]</sub><sup>-1</sup> h<sup>-1</sup>. <sup>a,b</sup> Determined from the ratio between total resonance integral and unsaturated end group intensity in the <sup>1</sup>H NMR spectra [26]. <sup>c</sup> Determined by size exclusion chromatography (SEC) vs. polystyrene standards. <sup>d</sup> Determined from <sup>1</sup>H NMR spectra [26]. <sup>e</sup> Polymerization conditions: Ni catalyst = 10 μmol (dissolved in 2 mL of o-dichlorobenzene), AlEt<sub>2</sub>Cl co-catalyst = 2 mmol, solvent = 50 mL toluene. <sup>f</sup> Low-molecular weight polyethylene oil recovered from the reaction mixture. <sup>g</sup> Solid polyethylene precipitated in methanol. <sup>h</sup> polymerization conditions: Ni catalyst = 10 μmol (dissolved in 2 mL of dichloromethane), AlEt<sub>2</sub>Cl co-catalyst = 2 mmol, solvent = 20 mL toluene.

The formation of polymer parts with various structures and molecular weights suggests that by using AlEt<sub>2</sub>Cl, numerous active species can be created in situ. To investigate the idea in detail, two polymerization runs were conducted at 0 °C under 1 atm of ethylene for 1 hour utilizing catalyst 1 and 2 activated by AlEt<sub>2</sub>Cl.

Acidified methanol was used to quench the reactions, after adding water, the reaction solution were recovered with dichloromethane, and the precipitate

formed was separated by a silica column and washed with hexane and then dichloromethane. The filtrate product was analyzed using  $^1\text{H NMR}$ , revealing the presence of both imine ligands and the respective amines formed via imine reduction. Notably, post-polymerization ligand adjustment was more significant for the aldimine catalyst 3 than for the ketimine catalyst 11, as for aldimine catalyst 2 produced 11% of the amine and ketimine catalyst 1 just 5%. Furthermore, repeating the experiment at a higher temperature ( $40^\circ\text{C}$ ) with the ketimine catalyst 1 resulted in the production of 22% of amine (Figure 46, Figure 47).

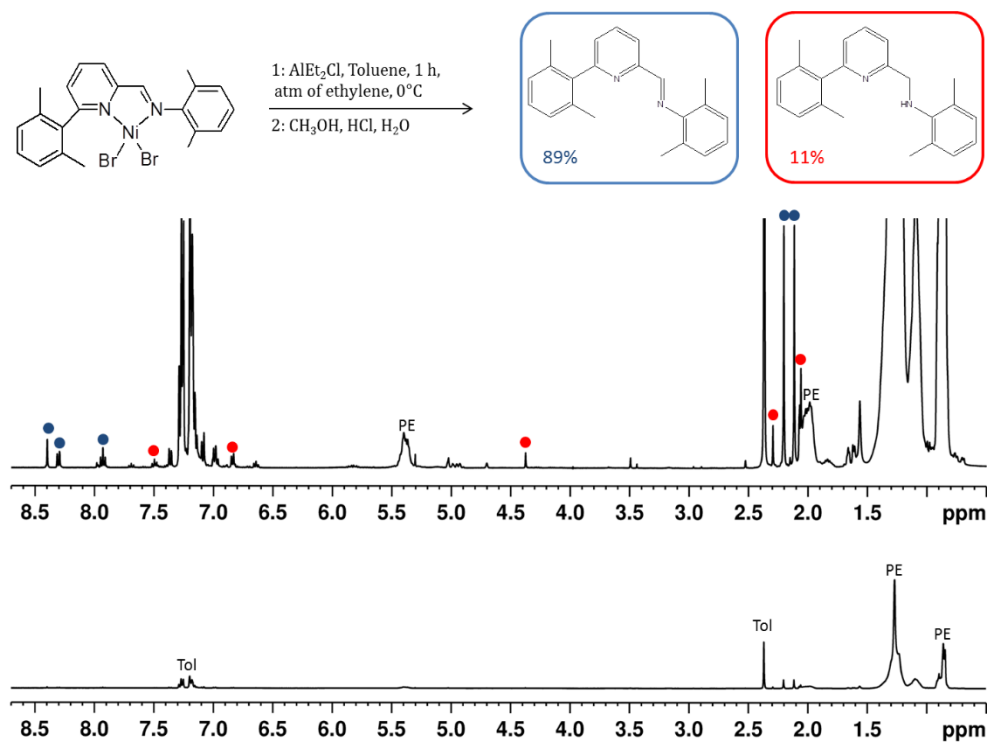


**Figure 46.**  $^1\text{H NMR}$  (CDCl<sub>3</sub>, T = 293 K) spectra of the products of reaction between complex 12 and  $\text{AlEt}_2\text{Cl}$  under ethylene pressure.

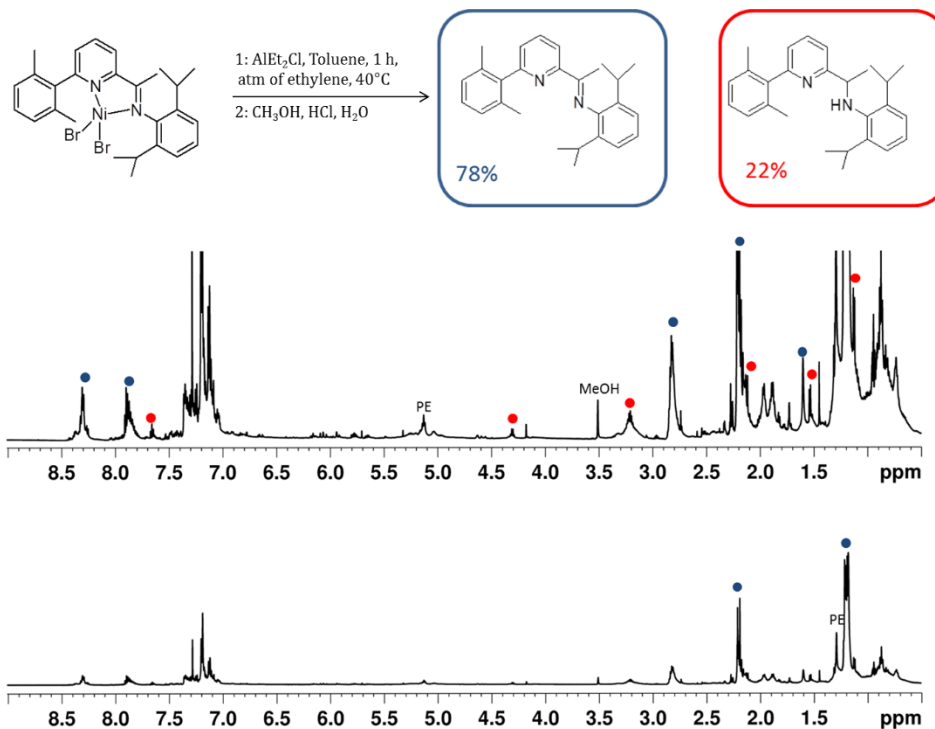


**Figure 47.**  $^1\text{H NMR}$  (CDCl<sub>3</sub>, T = 293 K) spectra of the products of reaction between complex 1 and  $\text{AlEt}_2\text{Cl}$  under ethylene pressure.

In accordance with the idea, control experiment without ethylene was performed, yielded in formation of the original imino and reduced amino ligands, as discovered in the presence of ethylene and an extra amine species carrying an ethyl group attached to the carbon in the alpha position in relation to the N atom (Figure 48) [27].



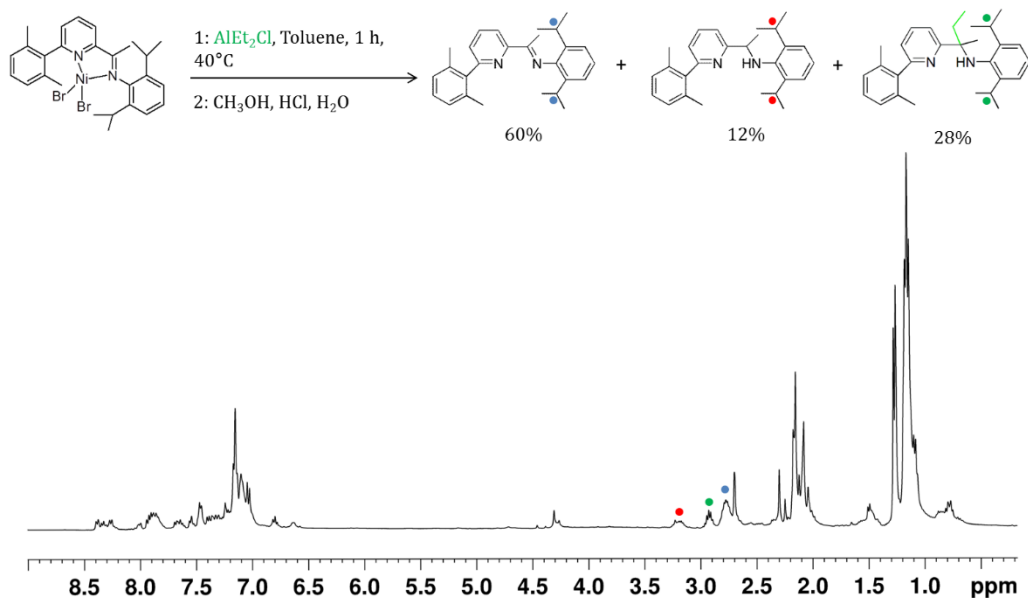


**Figure 48.**  $^1\text{H}$  NMR ( $\text{CDCl}_3$ ,  $T = 293\text{ K}$ ) spectrum of the products of reaction between complex 1 and  $\text{AlEt}_2\text{Cl}$  under nitrogen atmosphere, without ethylene.

Taking the preceding into consideration, we chose to synthesize the original amine Ni catalysts 11 and 12 with ligand structures identical to those of the imine complexes 10 and 1. The compounds were synthesized in high yields by allowing the amine ligands and dimethoxyethane nickel dibromide to react for 16 h at room temperature in  $\text{CH}_2\text{Cl}_2$ .

After activation with  $\text{AlEt}_2\text{Cl}$ , the pyridylamino complex 11 was used to polymerize ethylene at  $0^\circ\text{C}$  under an ethylene pressure of 50 atm, resulting in the unique formation of low molecular weight highly branched polyethylene oils (see run 10, Table 7). In comparison, the analogous pyridylimino catalyst 1 under

comparable condition (while using lower concentration, see the Experimental Section) resulted in the formation of a mixture of solid polyethylene and an oily fraction, with increased yield (run 1, Table 6). Pyridylamino complex 12 produced low molecular weight highly branched polyethylene oils under the same conditions, however in trace amounts (see run 11, Table 7). At  $T = 40^\circ \text{C}$  and 10 or 50 atm of ethylene pressures, catalysts 5 and 6 were also investigated; in all cases, low yields of hyperbranched polyethylene oils were obtained. Remarkably, the branching degree for both catalysts was larger at 50 atm than at 10 atm (runs 12 vs. 13 and 14 vs. 15), which is in contrast with all published results for Ni(II) catalysts generating branched polyethylenes via a "chain walking" process [1].

**Table 7.** Ethylene polymerization by aminopyridine complexes 11 and 12.

Run <sup>a</sup>	complex	Temperature (°C)	P (atm)	Yield (g)	Activity <sup>b</sup>	$M_n^c$ (kDa)	% Branches <sup>d</sup>
10	<b>14</b>	0	50	0.11	3.0	2.2	20.4
11	<b>15</b>	0	50	0.02	0.5	4.9	8.8
12	<b>14</b>	40	10	0.06	1.5	4.5	13.3
13	<b>14</b>	40	50	0.20	5.0	5.8	29.8
14	<b>15</b>	40	10	0.05	1.2	3.3	12.4
15	<b>15</b>	40	50	0.10	2.5	4.6	21.9

<sup>a</sup> Polymerization conditions: Ni catalyst = 10  $\mu\text{mol}$ ,  $\text{AlEt}_2\text{Cl}$  = 2 mmol, solvent = 20 mL toluene, time = 4 h. <sup>b</sup> Activity in  $\text{kg mol}_{[\text{Ni}]}^{-1} \text{h}^{-1}$ . <sup>c</sup> Determined from ratio between total resonance integral and unsaturated end group intensity in the  $^1\text{H}$  NMR spectra [26]. <sup>d</sup> Determined from  $^1\text{H}$  NMR spectra [26].

Ni(II) catalysts are well-known for their "chain-walking" mechanism of action which includes a series of  $\beta$ -hydride eliminations and reinsertions with inverted regiochemistry: this, results in a diverse composition of branches with different lengths incorporated into the polymer chain [1]. As previously documented in literature, the degree of branching is dependent on temperature, monomer pressure, and catalyst structure: higher polymerization temperatures, lower monomer pressure, and a larger steric bulk in the square-planar coordination sphere's axial positions increases the amount of branching [1, 9, 28].

However, the aforementioned framework cannot account for the simultaneous formation of the various macromolecules observed in the polymerization runs described above using these Ni(II) catalysts having aryliminopyridine ligands with bulky substituents at both the imino moiety and the 6-position of pyridine. On the other hand, there are numerous examples in the literature demonstrating that olefin polymerization catalysts based on imino complexes activated by aluminum alkyls can be modified in situ, resulting in a reduction of the imino functionality [29-31]. Thus, it is feasible to assume that under the analyzed conditions, numerous active species are created. Furthermore, our investigations investigating the outcome of the iminopyridine Ni(II) catalysts following the polymerization run revealed that the original ligands revealed partial transformation into the relevant aminopyridines. This observation provides support the multi-site nature of the catalyst systems, under special conditions.

To provide more evidence, two aminopyridine Ni(II) complexes (11 and 12) with structures identical to those of the iminopyridine complexes 1 and 2 were produced and analyzed. Although aminopyridine Ni(II) complexes have been

recently reported to be effective for ethylene polymerization catalysts [32, 33], applying aminopyridine complexes with aryl groups in the 6-position of the pyridine molecule, analogous to 11 and 12, only small quantities of uncharacterized oligomers were produced [33].

Polymerization results studied here indicate that, under identical conditions ( $T = 0^{\circ}\text{C}$ ,  $P = 50 \text{ atm}$ ), the aminopyridine catalysts yield only small amounts of hyperbranched polyethylene oils, whereas the iminopyridine analogs yield mixtures of various macromolecules, indicating feasible modification of the imino functionality. Surprisingly, for the aminopyridine complexes, increasing monomer pressure results in the formation of more branching polyethylenes, opposite to the typical behavior of Ni(II) catalysts. This feature is worth notable, as one of Brookhart's Ni(II) catalysts' major drawbacks for functional applications in the area of elastomeric materials acquired purely from ethylene (without addition of comonomers such as propene or 1-hexene) shows that the polymers formed at the high pressures desired by industrial processes are significantly linear.

## Chapter 3

### EXPERIMENTAL PART

#### 3.1 General Conditions

All procedures sensitive to air or moisture were performed under a nitrogen atmosphere using standard Schlenk techniques. Glassware used were dried in an oven at 120 °C overnight and exposed three times to vacuum–nitrogen cycles. Solvents were dried by refluxing with a drying agent (CaH<sub>2</sub> for dichloromethane and metallic sodium for toluene and *o*-dichlorobenzene) and distillation under nitrogen. Deuterated solvents were purchased from Aldrich and stored in the glovebox over 3 Å molecular sieves before use. All other reagents were purchased from Aldrich and used as received. Ethylene was purchased from SON and used without further purification.

The NMR spectra were recorded on a Bruker Avance 400, a Bruker 600 MHz Ascend 3 HD spectrometers and a Varian 500 MHz <sup>1</sup>H NMR spectra are referenced using the residual solvent peak at  $\delta$  7.26 for CDCl<sub>3</sub> and  $\delta$  6 for TCDE. <sup>13</sup>C NMR spectra are referenced using the residual solvent peak at  $\delta$  77.16 for CDCl<sub>3</sub> and  $\delta$  73.78 for TCDE. <sup>13</sup>C NMR spectra are referenced using the residual solvent peak at  $\delta$  77.16 for CDCl<sub>3</sub> and  $\delta$  73.78 for TCDE.

The molecular weights ( $M_n$  and  $M_w$ ) and the molecular mass distribution ( $M_w/M_n$ ) of the polymer samples were measured by Size Exclusion Chromatography (SEC) at 30°C, using THF as solvent, an eluent flow rate of 1

mL/min, and narrow polystyrene standards as reference. The measurements were performed on a Waters 1525 binary system equipped with a Waters 2414 RI detector using four Styragel columns (range 1 000–1 000 000 Å). Gramer

High-resolution mass spectra (HRMS) were carried out using a Bruker Solarix XR Fourier transform ion cyclotron resonance mass spectrometer (Bruker Daltonik GmbH, Bremen, Germany) equipped with a 7 T refrigerated actively-shielded superconducting magnet (Bruker Biospin, issembourg, France). The samples were ionized in positive ion mode using the ESI ion source (Bruker Daltonik GmbH, Bremen, Germany). The mass range was set to  $m/z$  150 – 3000. Mass calibration: The mass spectra were calibrated externally using a NaTFA solution in positive ion mode. A linear calibration was applied.

### **3.2 General procedure for ethylene homo- and copolymerizations at 6 atm**

Ethylene homo- and co-polymerizations at 6 atm were all carried out in a 250 mL Büchi glass autoclave equipped with a mechanical stirrer and a temperature probe. The reactor was kept under vacuum overnight at 80°C. In a typical run, the reactor vessel was charged under a nitrogen atmosphere with 100 mL of a toluene solution containing the Ni catalyst, the cocatalyst and, for the copolymerization, the MA comonomer. Then it was pressurized with ethylene and vented three times. The mixture was stirred at 40°C under constant ethylene pressure for 4 h and then the autoclave was vented, and the reaction mixture was poured into acidified methanol. The resulting solution was treated with hexane and water, then the organic layer was dried over MgSO<sub>4</sub>, filtered and the volatiles were distilled off in a rotavapor. The resulting oily residue was dried in vacuo overnight at 80°C.

### 3.3 General procedure for ethylene-methyl acrylate copolymerization at higher pressures

Ethylene copolymerizations at high pressures (10-50 atm) were carried out in a stainless steel autoclave equipped with a magnetic stirrer. The reactor was first dried overnight at 120°C in an oven, cooled under vacuum, then pressurized with ethylene and vented 3 times. The reactor was thermostated at 40 °C, charged with 20 ml of toluene, the solution of cocatalyst, catalyst and methyl acrylate, and then pressurized at the prescribed ethylene pressure. The mixture was stirred for 20 h under constant ethylene pressure and then poured into acidified methanol. The soluble copolymers were recovered as described above. Only in the case of runs 7 and 8, solid polymers precipitated in methanol and were recovered by filtration, washed with fresh methanol and dried in vacuo at 80 °C overnight.

### 3.4 Synthesis of ligands and complexes

**Ligand L1.** was synthesized as described in our previous literature [21, 25, 34, 35].

**(6-bromo-2-(2,6-diisopropylphenyl)ketiminopyridine)**                      2-Acetyl-6-bromopyridine (6.79 g, 34 mmol) was combined with 2,6-diisopropylaniline (6.02 g, 34 mmol) in 120 ml of anhydrous toluene containing 0.3 nm pore size molecular sieves (3g) as well as 8 mg of p-TsOH. The mixture was heated to 70°C under N<sub>2</sub> for 16 h. After solvent evaporation, a yellow solid was obtained. (6.79 g, 99% yield). <sup>1</sup>H NMR (CDCl<sub>3</sub>, 400 MHz, 25°C): δ 8.33 (d, J = 7.6 Hz, 1Hpyridine), 7.69 (t, J = 7.6 Hz, 1Hpyridine), 7.59 (d, J = 7.6 Hz, 1Hpyridine), 7.26-7.12 (m, 3Haryle), 2.71 (sept, J = 6.8 Hz, 2H, CH(CH<sub>3</sub>)<sub>2</sub>), 2.18(s, 3H, CH<sub>3</sub>).1.14 (d, J = 6.8 Hz, 12H, CH(CH<sub>3</sub>)<sub>2</sub>). <sup>13</sup>C NMR (CDCl<sub>3</sub>, 100.67 MHz,

25°C):  $\delta$  161.63 (-CH=N-), 155.62 (C), 148.05 (C), 142.00 (C), 139.15 (CH), 137.18 (CH), 129.96 (CH), 124.84 (2C), 123.22 (2CH), 120.03 (CH), 28.10 (CH(CH<sub>3</sub>)<sub>2</sub>), 22.59 (CH(CH<sub>3</sub>)<sub>2</sub>).

**6-(2,6-dimethylphenyl)-2-(2,6-diisopropylphenyl)ketiminopyridine (L1).** To a suspension of 6-bromo-2-(2,6-diisopropylphenyl)ketiminopyridine (2.87 g, 8.00 mmol) and Pd(PPh<sub>3</sub>)<sub>4</sub> (0.25 g, 0.22 mmol) in toluene (20 mL), aqueous 2.0 M Na<sub>2</sub>CO<sub>3</sub> (10 mL) and 2,6-dimethyl-phenylboronic acid (1.80 g, 12.00 mmol) dissolved in methanol (8 mL) were subsequently added. After refluxing the suspension for 16 h, a 2.0 M aqueous solution of Na<sub>2</sub>CO<sub>3</sub> (50 mL) and CH<sub>2</sub>Cl<sub>2</sub> (100 mL) were added to the solution after cooling to room temperature. The aqueous phase was separated and extracted with CH<sub>2</sub>Cl<sub>2</sub> (30 mL), and the combined organic extracts were dried using Na<sub>2</sub>SO<sub>4</sub>. Further purification by a silica gel column chromatography, using 9:1 hexane/ethyl acetate as the eluent, gave the title compounds as a brown solid (1.40 g, 47% yield).

<sup>1</sup>H NMR (400 MHz, CDCl<sub>3</sub>, 25°C): 8.26 (d, J = 7.6 Hz, 1Hpyridine), 7.90 (t, J = 7.6 Hz, 1Hpyridine), 7.34 (d, J = 7.6, 1Hpyridine), 2.82 [sept, J = 6.8 Hz, 2H, CH(CH<sub>3</sub>)<sub>2</sub>], 2.18 (s, 3H, CH<sub>3</sub> aryl), 1.19 [d, J = 6.8 Hz, 12H, CH(CH<sub>3</sub>)<sub>2</sub>]. <sup>13</sup>C NMR (100.67 MHz, CDCl<sub>3</sub>, 25°C):  $\delta$  = 164.39 (-N=CH-), 159.97 (C), 154.72 (C), 154.67 (C), 154.62 (C), 150.36 (C), 139.99 (C), 137.62 (2C), 136.61 (CH), 135.84 (2C), 128.84 (CH), 123.64 (2CH), 119.78 (CH), 119.78 (CH), 30.67 [CH(CH<sub>3</sub>)<sub>2</sub>], 20.11 [CH(CH<sub>3</sub>)<sub>2</sub>], 20.08 [CH(CH<sub>3</sub>)<sub>2</sub>], 18.88 (CH<sub>3</sub>), 18.01 (CH<sub>3</sub>).



**Ligand L2.** Analogously to the preparation of ligand L1, ligand L2 was synthesized from 6-Bromo-2-pyridinecarboxaldehyde and 2,6-dimethylaniline (1.48 g, 50% yield).

$^1\text{H}$  NMR (400 MHz,  $\text{CDCl}_3$ ,  $25^\circ\text{C}$ ):  $\delta$  = 8.38 (s, 1 H,  $-\text{N}=\text{CH}-$ ), 8.27 (d,  $J$  = 7.6 Hz, 1Hpyridine), 7.90 (t,  $J$  = 7.6 Hz, 1Hpyridine), 7.35 (d,  $J$  = 7.6, 1Hpyridine), 2.28 [d, 3H,  $(\text{CH}_3)_2$ ], 2.10 (d, 3H,  $\text{CH}_3$ ).  $^{13}\text{C}$  NMR (100.67 MHz,  $\text{CDCl}_3$ ,  $25^\circ\text{C}$ ):  $\delta$  = 164.39 ( $-\text{N}=\text{CH}-$ ), 159.97 (C), 154.72 (C), 154.67 (C), 150.36 (C), 139.99(2C), 137.62 (2C), 136.61 (CH), 128.84 (CH), 123.64 (CH), 119.78 (2CH), 20.11 ( $\text{CH}_3$ ), 18.88 ( $\text{CH}_3$ ).

### **Ligand L3.**

**6-methyl-2-(2,6-diisopropylphenyl)iminopyridine (L3).** To a solution of 6-Methylpyridine-2-carboxaldehyde (5.2 mmol, 0.64 g) in dry methanol, 2,6-diisopropylaniline (5.2 mmol, 0.921g) and 8 mg of p-TsOH were added. Product was crystalized in methanol at  $-20^\circ\text{C}$ . (0.58 g, 90% yield).

$^1\text{H}$  NMR (400 MHz,  $\text{CDCl}_3$ ,  $25^\circ\text{C}$ ):  $\delta$  = 8.38 (s, 1 H,  $-\text{N}=\text{CH}-$ ), 8.20 (d,  $J$  = 7.6 Hz, 1Hpyridine), 7.86 (t,  $J$  = 7.6 Hz, 1Hpyridine), 7.38 (d,  $J$  = 7.6, 1Hpyridine), 3.10 [sept,  $J$  = 6.8Hz, 2H,  $\text{CH}(\text{CH}_3)_2$ ], 2.74 (s, 1 H, CH), 1.26 [d,  $J$  = 6.8Hz, 12H,  $\text{CH}(\text{CH}_3)_2$ ].  $^{13}\text{C}$  NMR (100.67 MHz,  $\text{CDCl}_3$ ,  $25^\circ\text{C}$ ):  $\delta$  = 163.98 ( $-\text{N}=\text{CH}-$ ), 158.63 (C), 154.05 (C), 148.66 (C), 137.56 (2C), 136.47 (CH), 125.66 (CH), 124.97 (CH), 122.59 (2CH), 117.94 (CH), 27.65 [ $\text{CH}(\text{CH}_3)_2$ ], 23.98 [ $\text{CH}(\text{CH}_3)_2$ ], 23.10 ( $\text{CH}_3$ ).

**Ligand L4.** Analogously to the preparation of ligand L3, ligand L4 was synthesized from 2-acetyl-6-methylpyridine.  $^1\text{H NMR}$  (400 MHz,  $\text{CDCl}_3$ ,  $25^\circ\text{C}$ ):  $\delta = 8.20$  (d,  $J = 7.6$  Hz,  $^1\text{Hpyridine}$ ),  $7.86$  (t,  $J = 7.6$  Hz,  $^1\text{Hpyridine}$ ),  $7.38$  (d,  $J = 7.6$ ,  $^1\text{Hpyridine}$ ),  $3.10$  [sept,  $J = 6.8\text{Hz}$ , 2H,  $\text{CH}(\text{CH}_3)_2$ ],  $2.74$  (s, 1 H, CH),  $2.17$  (s, 3H,  $\text{CH}_3$ ),  $1.26$  [d,  $J = 6.8\text{Hz}$ , 12H,  $\text{CH}(\text{CH}_3)_2$ ].  $^{13}\text{C NMR}$  (100.67 MHz,  $\text{CDCl}_3$ ,  $25^\circ\text{C}$ ):  $\delta = 163.98$  (-N=CH-),  $158.63$  (C),  $154.05$  (C),  $148.66$  (C),  $137.56$  (2C),  $136.47$  (CH),  $125.66$  (CH),  $124.97$  (CH),  $122.59$  (2CH),  $117.94$  (CH),  $27.65$  [ $\text{CH}(\text{CH}_3)_2$ ],  $23.98$  [ $\text{CH}(\text{CH}_3)_2$ ],  $23.10$  ( $\text{CH}_3$ ).

**Preparation of complexes.** All complexes were prepared analogously from  $[(\text{DME})\text{NiBr}_2]$  and the corresponding ligand in dichloromethane. The reaction mixture was stirred at room temperature for 24 h. The solvent was removed under vacuum and the residues were washed with dry hexane and dried. ESI(+) -MS analysis:[603.05]; (L1-Ni-Br+) 523.15.  
ESI(+) -MS analysis:[532.92]; (L2-Ni-Br+) 453.03.  
ESI(+) -MS analysis:[498.91]; (L3-Ni-Br+) 419.04 (Figure 50, Figure 51, Figure 52).

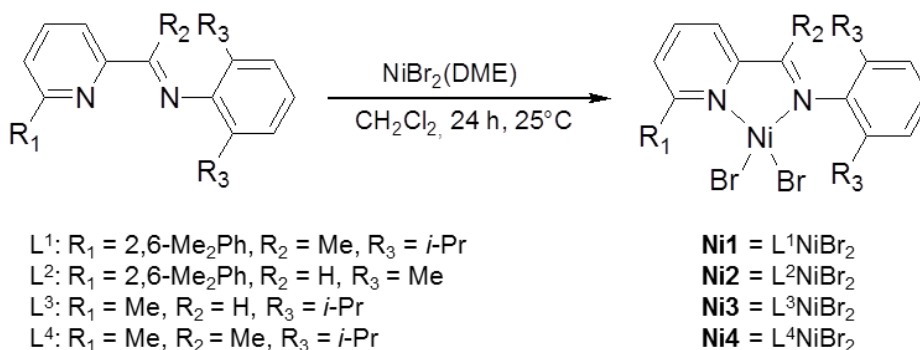


**Figure 49.** Synthesis of the Ni-complexes Ni1-Ni4.

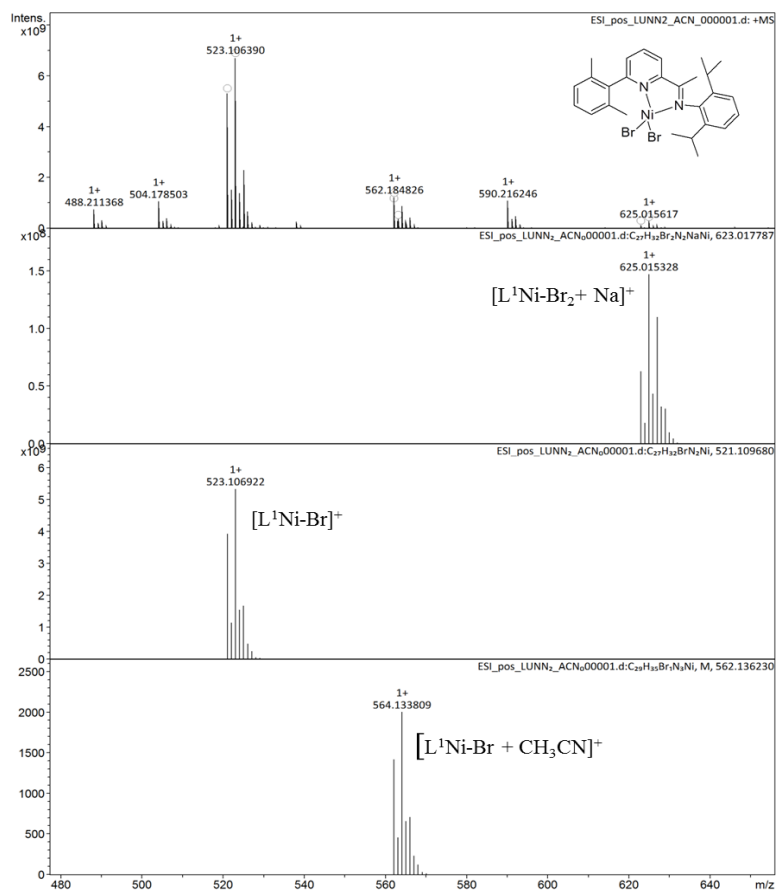


**Figure 50.** HR ESI Mass spectrum of complex Ni1 ( $L^1NiBr_2$ ).

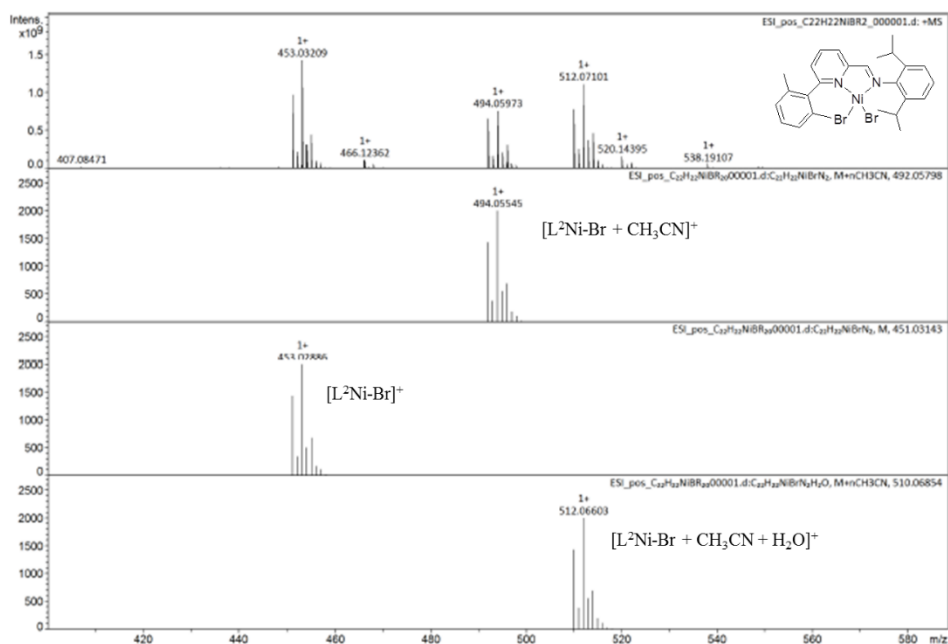


**Figure 51.** HR ESI Mass spectrum of complex **Ni2** (L<sup>2</sup>NiBr<sub>2</sub>).

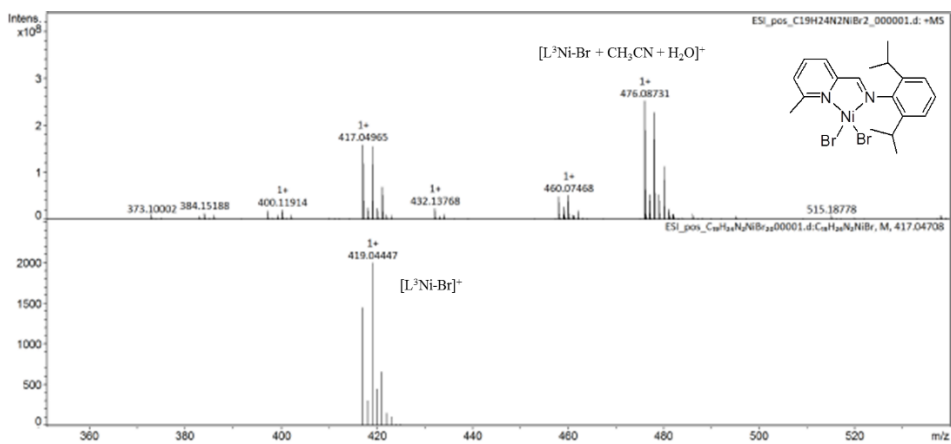


**Figure 52.** HR ESI Mass spectrum of complex **Ni3** (L<sub>3</sub>NiBr<sub>2</sub>).

Ligand **L10** and complex **C10** were synthesized as described in literature [20].

**Complex 10.** To a solution of **L10** (0.32 mmol, 0.12g) in dry dichloromethane, [(DME)NiBr<sub>2</sub>] (0.31 mmol, 0.1g) was added. The reaction mixture was stirred at room temperature for 24 h. The solvent was removed under vacuum and the residues were washed with dry hexane and dried to obtain a green solid (0.15 g, 90% yield).

Ligands **L11** and **L12** were synthesized as described in literature [36].

Complexes **C11** and **C12** were synthesized as described in literature [36].

## CONCLUSION

The investigation into copolymerizing olefins by Ni(II) complexes bearing pyridylimine ligands was achieved in this study. The complexes, in the presence of a proper activating agent, were found to generate active catalysts for the ethylene-methyl acrylate copolymerization leading to hyperbranched copolymers with the polar monomer inserted in a variety of modes. The nature of the pyridylimine ligand determines catalyst activity, polymer molecular weight, and content of inserted MA. The ligand nature does not affect the manner of incorporation of MA that is dictated by both the activating agent and the solvent used to dissolve the nickel precatalyst: selective in-chain MA insertion occurs when the activator is AlEt<sub>2</sub>Cl and the precatalyst is dissolved in o-dichlorobenzene, while a variety of insertion modes occur in the presence of dichloromethane or AlMe<sub>3</sub>/B(C<sub>6</sub>F<sub>5</sub>)<sub>3</sub>/[Ph<sub>3</sub>C][B(C<sub>6</sub>F<sub>5</sub>)<sub>4</sub>] cocatalyst.

On the other hand we have tested other types of nickel complexes containing 2-((arylimino)ethyl)pyridine for copolymerizing of ethylene with methyl acrylate. In all cases the complexes obtained solid polymers with different amounts of methyl acrylate incorporation based on substituents containing electron-donating or electron-withdrawing. For those ones with electron-donating, the amount of obtained copolymer is significantly more than those having electron withdrawing substituents.

Moreover we reasoned that increasing the steric bulk at the arylimino moiety could afford E-MA copolymers with higher molecular weight and lower branching, resulting in the formation of solid crystalline products instead of oils. Thus, we reported the copolymerization of ethylene and methyl acrylate

promoted by the dibenzocycloheptyl-substituted aryliminopyridyl Ni(II) complexes.

Furthermore, the nickel complexes containing pyridylimine ligands were tested under homopolymerization of ethylene resulting in different amounts of both solid and oily products.

In fact, our experiments analyzing the fate of the iminopyridine Ni(II) catalysts after the polymerization run showed the partial transformation of the original ligands in the corresponding aminopyridines. This finding supports the multi-site nature of our catalyst systems. The polymerization results have shown that, the aminopyridine complexes produce only low amounts of hyperbranched polyethylene oils, while the iminopyridine affords mixtures of different types of macromolecules, suggesting the possible modification of the imino functionality. However, for the aminopyridine complexes more branched polyethylenes are produced at higher monomer pressure, at variance with the usual behavior of Ni(II) catalysts. The latter could be an interesting feature, since one of the main limitations of Brookhart's Ni(II) catalysts for practical applications in the field of elastomeric materials obtained by ethylene feed only (without the need of comonomers such as propene or 1-hexene) is the fact that the polymers obtained under the high pressures required by the industrial processes are substantially linear.

## References

- [1] S.D. Ittel, L.K. Johnson, M. Brookhart, Late-metal catalysts for ethylene homo- and copolymerization, *Chemical Reviews* 100(4) (2000) 1169-1204.
- [2] L. Guo, H. Gao, Q. Guan, H. Hu, J. Deng, J. Liu, F. Liu, Q. Wu, Substituent effects of the backbone in  $\alpha$ -diimine palladium catalysts on homo- and copolymerization of ethylene with methyl acrylate, *Organometallics* 31(17) (2012) 6054-6062.
- [3] S. Zhong, Y. Tan, L. Zhong, J. Gao, H. Liao, L. Jiang, H. Gao, Q. Wu, Precision synthesis of ethylene and polar monomer copolymers by palladium-catalyzed living coordination copolymerization, *Macromolecules* 50(15) (2017) 5661-5669.
- [4] S. Dai, S. Zhou, W. Zhang, C. Chen, Systematic investigations of ligand steric effects on  $\alpha$ -diimine palladium catalyzed olefin polymerization and copolymerization, *Macromolecules* 49(23) (2016) 8855-8862.
- [5] F. Zhai, J.B. Solomon, R.F. Jordan, Copolymerization of ethylene with acrylate monomers by amide-functionalized  $\alpha$ -diimine Pd catalysts, *Organometallics* 36(9) (2017) 1873-1879.
- [6] A. Meduri, T. Montini, F. Ragaini, P. Fornasiero, E. Zangrando, B. Milani, Palladium-Catalyzed Ethylene/Methyl Acrylate Cooligomerization: Effect of a New Nonsymmetric  $\alpha$ -Diimine, *ChemCatChem* 5(5) (2013) 1170-1183.
- [7] V. Rosar, T. Montini, G. Balducci, E. Zangrando, P. Fornasiero, B. Milani, Palladium-Catalyzed Ethylene/Methyl Acrylate Co-Oligomerization: The Effect of a New Nonsymmetrical  $\alpha$ -Diimine with the 1, 4-Diazabutadiene Skeleton, *ChemCatChem* 9(17) (2017) 3402-3411.
- [8] V. Rosar, A. Meduri, T. Montini, P. Fornasiero, E. Zangrando, B. Milani, The contradictory effect of the methoxy-substituent in palladium-catalyzed ethylene/methyl acrylate cooligomerization, *Dalton Transactions* 47(8) (2018) 2778-2790.
- [9] L.K. Johnson, C.M. Killian, M. Brookhart, New Pd (II)- and Ni (II)-based catalysts for polymerization of ethylene and  $\alpha$ -olefins, *Journal of the American Chemical Society* 117(23) (1995) 6414-6415.
- [10] K.E. Allen, J.s. Campos, O. Daugulis, M. Brookhart, Living polymerization of ethylene and copolymerization of ethylene/methyl acrylate using "sandwich" diimine palladium catalysts, *ACS Catalysis* 5(1) (2015) 456-464.
- [11] Y. Liao, Y. Zhang, L. Cui, H. Mu, Z. Jian, Pentaipicyenyl substituents in insertion polymerization with  $\alpha$ -diimine nickel and palladium species, *Organometallics* 38(9) (2019) 2075-2083.



- [12] R. Wang, M. Zhao, C. Chen, Influence of ligand second coordination sphere effects on the olefin (co) polymerization properties of  $\alpha$ -diimine Pd (II) catalysts, *Polymer Chemistry* 7(23) (2016) 3933-3938.
- [13] S. Takano, D. Takeuchi, K. Osakada, N. Akamatsu, A. Shishido, Dipalladium catalyst for olefin polymerization: Introduction of acrylate units into the main chain of branched polyethylene, *Angewandte Chemie* 126(35) (2014) 9400-9404.
- [14] A. Nakamura, T.M. Anselment, J. Claverie, B. Goodall, R.F. Jordan, S. Mecking, B. Rieger, A. Sen, P.W. Van Leeuwen, K. Nozaki, Ortho-phosphinobenzenesulfonate: A superb ligand for palladium-catalyzed coordination–insertion copolymerization of polar vinyl monomers, *Accounts of chemical research* 46(7) (2013) 1438-1449.
- [15] Y. Ota, S. Ito, J.-i. Kuroda, Y. Okumura, K. Nozaki, Quantification of the steric influence of alkylphosphine–sulfonate ligands on polymerization, leading to high-molecular-weight copolymers of ethylene and polar monomers, *Journal of the American Chemical Society* 136(34) (2014) 11898-11901.
- [16] T.R. Younkin, E.F. Connor, J.I. Henderson, S.K. Friedrich, R.H. Grubbs, D.A. Bansleben, Neutral, single-component nickel (II) polyolefin catalysts that tolerate heteroatoms, *Science* 287(5452) (2000) 460-462.
- [17] Z. Chen, M.D. Leatherman, O. Daugulis, M. Brookhart, Nickel-catalyzed copolymerization of ethylene and vinyltrialkoxysilanes: catalytic production of cross-linkable polyethylene and elucidation of the chain-growth mechanism, *Journal of the American Chemical Society* 139(44) (2017) 16013-16022.
- [18] Z. Chen, M. Brookhart, Exploring ethylene/polar vinyl monomer copolymerizations using Ni and Pd  $\alpha$ -diimine catalysts, *Accounts of chemical research* 51(8) (2018) 1831-1839.
- [19] T. Liang, C. Chen, Position makes the difference: electronic effects in nickel-catalyzed ethylene polymerizations and copolymerizations, *Inorganic chemistry* 57(23) (2018) 14913-14919.
- [20] Z. Saki, I. D’Auria, A. Dall’Anese, B. Milani, C. Pellecchia, Copolymerization of Ethylene and Methyl Acrylate by Pyridylimino Ni (II) Catalysts Affording Hyperbranched Poly (ethylene-co-methyl acrylate) s with Tunable Structures of the Ester Groups, *Macromolecules* 53(21) (2020) 9294-9305.
- [21] T.V. Laine, U. Piironen, K. Lappalainen, M. Klinga, E. Aitola, M. Leskelä, Pyridinylimine-based nickel (II) and palladium (II) complexes: preparation, structural characterization and use as alkene polymerization catalysts, *Journal of Organometallic Chemistry* 606(2) (2000) 112-124.
- [22] Y. Zhang, C. Wang, S. Mecking, Z. Jian, Ultrahigh branching of main-chain-functionalized polyethylenes by inverted insertion selectivity, *Angewandte Chemie International Edition* 59(34) (2020) 14296-14302.

- [23] A. Dall'Anese, V. Rosar, L. Cusin, T. Montini, G. Balducci, I. D'Auria, C. Pellecchia, P. Fornasiero, F. Felluga, B. Milani, Palladium-catalyzed ethylene/methyl acrylate copolymerization: moving from the acenaphthene to the phenanthrene skeleton of  $\alpha$ -diimine ligands, *Organometallics* 38(19) (2019) 3498-3511.
- [24] N.D. Contrella, J.R. Sampson, R.F. Jordan, Copolymerization of ethylene and methyl acrylate by cationic palladium catalysts that contain phosphine-diethyl phosphonate ancillary ligands, *Organometallics* 33(13) (2014) 3546-3555.
- [25] I. D'Auria, S. Milione, T. Caruso, G. Balducci, C. Pellecchia, Synthesis of hyperbranched low molecular weight polyethylene oils by an iminopyridine nickel (II) catalyst, *Polymer Chemistry* 8(41) (2017) 6443-6454.
- [26] T. Wiedemann, G. Voit, A. Tchernook, P. Roesle, I. Göttker-Schnetmann, S. Mecking, Monofunctional hyperbranched ethylene oligomers, *Journal of the American Chemical Society* 136(5) (2014) 2078-2085.
- [27] V.C. Gibson, C. Redshaw, A.J. White, D.J. Williams, Synthesis and structural characterisation of aluminium imino-amide and pyridyl-amide complexes: Bulky monoanionic N, N chelate ligands via methyl group transfer, *Journal of organometallic chemistry* 550(1-2) (1998) 453-456.
- [28] V.C. Gibson, S.K. Spitzmesser, Advances in non-metallocene olefin polymerization catalysis, *Chemical reviews* 103(1) (2003) 283-316.
- [29] J. Saito, M. Onda, S. Matsui, M. Mitani, R. Furuyama, H. Tanaka, T. Fujita, Propylene Polymerization with Bis (phenoxy-imine) Group-4 Catalysts Using *i*Bu<sub>3</sub>Al/Ph<sub>3</sub>CB (C<sub>6</sub>F<sub>5</sub>)<sub>4</sub> as a Cocatalyst, *Macromolecular rapid communications* 23(18) (2002) 1118-1123.
- [30] Y. Suzuki, N. Kashiwa, T. Fujita, Synthesis and Ethylene Polymerization Behavior of a New Titanium Complex Having Two Imine-Phenoxy Chelate Ligands, *Chemistry letters* 31(3) (2002) 358-359.
- [31] A.V. Prasad, H. Makio, J. Saito, M. Onda, T. Fujita, Highly isospecific polymerization of propylene with bis (phenoxy-imine) Zr and Hf complexes using *i*Bu<sub>3</sub>Al/Ph<sub>3</sub>CB (C<sub>6</sub>F<sub>5</sub>)<sub>4</sub> as a cocatalyst, *Chemistry letters* 33(3) (2004) 250-251.
- [32] S. Zai, F. Liu, H. Gao, C. Li, G. Zhou, S. Cheng, L. Guo, L. Zhang, F. Zhu, Q. Wu, Longstanding living polymerization of ethylene: substituent effect on bridging carbon of 2-pyridinemethanamine nickel catalysts, *Chemical communications* 46(24) (2010) 4321-4323.
- [33] S. Zai, H. Gao, Z. Huang, H. Hu, H. Wu, Q. Wu, Substituent effects of pyridine-amine nickel catalyst precursors on ethylene polymerization, *ACS Catalysis* 2(3) (2012) 433-440.
- [34] Q. Dai, X. Jia, F. Yang, C. Bai, Y. Hu, X. Zhang, Iminopyridine-based cobalt (II) and nickel (II) complexes: Synthesis, characterization, and their catalytic behaviors for 1, 3-butadiene polymerization, *Polymers* 8(1) (2016) 12.

[35] C.A. Figueira, P.S. Lopes, C.S. Gomes, J.C. Gomes, L.F. Veiros, F. Lemos, P.T. Gomes, Neutral mono (5-aryl-2-iminopyrrolyl) nickel (II) complexes as precatalysts for the synthesis of highly branched ethylene oligomers: Preparation, molecular characterization, and catalytic studies, *Organometallics* 38(3) (2018) 614-625.

[36] I. D'Auria, M.C. D'Alterio, G. Talarico, C. Pellecchia, Alternating copolymerization of CO<sub>2</sub> and cyclohexene oxide by new pyridylamidozinc (II) catalysts, *Macromolecules* 51(23) (2018) 9871-9877.